Colloquium: Phononic thermal properties of two-dimensional materials

Xiaokun Gu

Institute of Engineering Thermophysics, School of Mechanical Engineering, Shanghai Jiao Tong University, Shanghai, China 200240 and Department of Mechanical Engineering, University of Colorado, Boulder, Colorado 80309, USA

Yujie Wei*

LNM, Institute of Mechanics, Chinese Academy of Sciences, Beijing, China, 100190

Xiaobo Yin

Department of Mechanical Engineering, University of Colorado, Boulder, Colorado 80309, USA and Materials Science and Engineering Program, University of Colorado, Boulder, Colorado 80309, USA

Baowen Li†

Department of Mechanical Engineering, University of Colorado, Boulder, Colorado 80309, USA

Ronggui Yang‡

Department of Mechanical Engineering, University of Colorado, Boulder, Colorado 80309, USA and Materials Science and Engineering Program, University of Colorado, Boulder, Colorado 80309, USA

(published 13 November 2018)

Following the emergence of many novel two-dimensional (2D) materials beyond graphene, interest has grown in exploring implications for fundamental physics and practical applications ranging from electronics, photonics, and phononics to thermal management and energy storage. In this Colloquium, a summary and comparison are given of the phonon properties, such as phonon dispersion and relaxation time, of pristine 2D materials with single-layer graphene to understand the role of crystal structure and dimension on thermal conductivity. A comparison is made of the phonon properties, contrasting idealized 2D crystals, realistic 2D crystals, and 3D crystals, and synthesizing this to develop a physical picture of how the sample size of 2D materials affects their thermal conductivity. The effects of geometry such as the number of layers and the nanoribbon width, together with the presence of defects, mechanical strain, and substrate interactions on the thermal properties of 2D materials are discussed. Intercalation affects both the group velocities and phonon relaxation times of layered crystals and thus tunes the thermal conductivity along both the through-plane and basal-plane directions. This Colloquium concludes with a discussion of the challenges in theoretical and experimental studies of thermal transport in 2D materials. The rich and special phonon physics in 2D materials make them promising candidates for exploring novel phenomena such as topological phonon effects and applications such as phononic quantum devices.

DOI: 10.1103/RevModPhys.90.041002

CONTENTS

*yujie_wei@lnm.imech.ac.cn
†Baowen.Li@Colorado.Edu
‡Ronggui.Yang@Colorado.Edu

I. INTRODUCTION

A thorough understanding of heat conduction, on the one hand, is of primary importance for fundamental research such as constructing microscopic pictures for macroscopic irreversible heat transfer, and, on the other hand, provides a theoretical basis for thermal energy control and management. The latter is crucial in our daily life, ranging from thermal management of electronic devices such as smart phones and power inverters in hybrid or all electric vehicles to power generation and energy utilization processes. In the macroscopic world, thermal conductivity is used as an indicator for the heat conducting capability of a material, implying that the phenomenological Fourier's law of heat conduction, which states that the heat flux is proportional to the temperature gradient, is valid.

With the rapid development of novel materials, in particular, low-dimensional materials such as quasi-one-dimensional (1D) nanowires, nanotubes, polymer fibers, and two-dimensional (2D) materials, such as graphene and transition metal dichalcogenides, one may ask: is Fourier's law of heat conduction (which describes diffusive transport of energy carriers) still valid in such low-dimensional materials? Answering this question is not trivial: it not only enriches our understanding of the nature of heat conduction but also may provide theoretical guidelines for applications of low-dimensional materials.

In the last few decades, we have witnessed important progress in this direction, resulting from the efforts made by physicists, mathematicians, and engineers. First of all, important progress in understanding of phonon transport in (quasi-) 1D systems has been achieved. Through many intensive numerical simulations (Lepri, Livi, and Politi, 2003, Dhar, 2008, Lepri, Livi, and Politi, 2016) and mathematical proofs (Prosen and Campbell, 2000),[1] thermal conductivity is not found to be an intensive property. Rather, thermal conductivity is divergent with system size in many 1D momentum conserved lattices and toy models [a more detailed discussion is given by Sato (2016)]. Different approaches such as hydrodynamics and renormalization group theory (Narayan and Ramaswamy, 2002; Mai and Narayan, 2006), mode coupling theory (Lepri, 1998; Lepri, Livi, and Politi, 1998), and Peierls-Boltzmann transport theory (Pereverzev, 2003) have been employed to show that the thermal conductivity follows $\kappa \sim L^{\varsigma}$, where L is the sample length and the exponent ς varies from system to system. This divergent thermal conductivity is shown to be connected with superdiffusion of phonons (S. Liu *et al.*, 2014).

The phononic thermal conduction in a quasi-1D system might not be the same as that in 1D lattice and toy models, because the atoms in the quasi-1D nanostructures can vibrate in the three-dimensional (3D) real space. However, anomalous thermal conduction behavior has also been observed in numerical simulations for carbon nanotubes (Maruyama, 2002; Zhang and Li, 2005), nanowires (Yang, Zhang, and Li, 2010), and polymer chains (Henry and Chen, 2008, 2009; Liu and Yang, 2012). It has been pointed out (Mingo and Broido, 2005) that if only the first-order three-phonon scatterings are considered, the thermal conductivity of nanotubes is indeed divergent with length, where the exponent ς has a value between $1/3$ and $1/2$. If the three-phonon scattering to second order is included in the calculations, the thermal conductivity converges to a finite value, but for very long nanotubes. This theoretical prediction has not yet been experimentally confirmed.

These theoretical and numerical studies have been naturally extended to 2D systems, although the studies are much more challenging as the degrees of freedom are significantly increased. The mode coupling theory (Ernst, Hauge, and Van Leeuwen, 1971, 1976a, 1976b; Lepri, Livi, and Politi, 2003), renormalization theory (Narayan and Ramaswamy, 2002), and numerical simulations (Lippi and Livi, 2000; Yang, Grassberger, and Hu, 2006; Xiong *et al.*, 2010; Wang, Hu, and Li, 2012) show that thermal conductivity in

[1]Note that later development found that momentum conservation does not necessarily mean an anomalous energy transport. For example, in the rotator model (Gendelman and Savin, 2000; Giardina *et al.*, 2000), although the angular momentum is conserved, the system demonstrates a finite thermal conductivity. However, further analysis found that this model does not support a nonvanishing pressure, and thus the infinite-wavelength phonons cannot carry any energy current. Recent numerical works also showed that in some momentum conserved 1D system with asymmetric interparticle potential, the thermal conductivity is finite (Zhong *et al.*, 2012; Chen *et al.*, 2016). It was later demonstrated that this seemingly convergent thermal conductivity is a finite size effect. When the system size becomes larger, the system shows again a divergent thermal conductivity (Wang, Hu, and Li, 2013; Das, Dhar, and Narayan, 2014; Savin and Kosevich, 2014). More recent works by Gendelman and Savin (2014) and Sato (2016) showed that in 1D momentum conserved systems, thermally activated dissociation and increased pressure can make the thermal transport normal.

2D anharmonic lattices diverges logarithmically with system size ($L \times L$), namely, $\kappa \sim \log(L)$. However, a rigorous mathematical proof from the fundamental symmetry of the system and fundamental law of conservation such as in 1D systems (Prosen and Campbell, 2000) is still lacking for 2D systems.

On the other hand, the novel 2D materials exemplified by graphene provide a great playground for scientists and engineers. In particular, the pioneering experimental measurements using the optothermal Raman method (Balandin *et al.*, 2008) showed that single-layer graphene may have a thermal conductivity between 2000 and 5000 W/mK at room temperature, even higher than that for diamond. This result has inspired many studies aiming at both understanding its underlying physics and exploring potential applications for heat exchangers and thermal management. Notably, those studies on phonon transport and thermal conductivity of graphene have laid a solid foundation for other emerging 2D materials, as reviewed by Balandin (2011), Nika and Balandin (2012, 2017), Pop, Varshney, and Roy (2012), Sadeghi, Pettes, and Shi (2012), Wang *et al.* (2014), Xu, Li, and Duan (2014), and Li *et al.* (2017).

Over the past decade, many novel 2D materials have emerged. Some of them have been shown to have similar or even superior electronic and optical properties than graphene and are proposed for a wide range of applications, such as field-effect transistors, light-emitting diodes, spintronics and valleytronics, topological insulators, catalysts, and energy storage. Understanding phononic thermal properties of such 2D materials could be very important for the design of novel 2D materials-enabled applications. However, most of these 2D materials are different from the "one-atom-thick" single-layer graphene, making the direct application of existing knowledge of graphene to other 2D materials questionable.

Controlling the thermal properties of 2D materials could enable new generations of thermoelectric materials, thermal insulators, and even phononic computing devices. The best thermoelectric materials, such as Bi_2Te_3-based alloys, are indeed layered materials. The diversity of 2D materials could lead to novel thermoelectric materials and fully dense superior thermal insulators with ultralow thermal conductivity by manipulating phonon mismatch between different layers of 2D materials. 2D materials may offer a novel platform to realize phonon thermal diodes, phonon transistors, topological phonon insulators, and even quantum memories and quantum sensors.

With the rapid discovery of novel 2D materials, and the increasing number of papers on the phonon and thermal properties of 2D materials, it is desirable to have a comprehensive picture about the state of the art of this field. Indeed, there are already quite a few recent review articles on distinct aspects of the thermal properties of 2D materials in addition to the aforementioned reviews on graphene: Wang *et al.* (2017) summarized the progress of measurement methods, and Xu, Chen, and Li (2016) provided a critical review on the advantage and disadvantage of existing numerical and experimental techniques and the respective challenging issues. While Zhang and Zhang (2017) focused more on the cutting-edge thermal devices such as thermal diodes and thermal modulators with graphene and MoS_2, Qin and Hu (2016) reviewed the diversity of thermal properties in other 2D materials.

In this Colloquium, we aim to provide a physical picture of how phonon scattering in 2D materials influences their thermal transport properties. This Colloquium not just summarizes the existing results (including numerical, theoretical, and experimental), but gives a pedagogical introduction to the physical picture of phonon scattering and thermal properties in both pristine 2D materials and their use in practical applications. The following fundamental questions will be answered:

(a) Can phonons in a suspended single-layer 2D material undergo diffusive motions that lead to a normal heat conduction, i.e., is the thermal conductivity independent of dimensions such as width and length? Since suspended single-layer 2D materials are very fragile and not easy to manipulate, they might not be suitable for many practical applications. A quite logical step is to substitute them with multilayer thin films. How does the interlayer interaction affect the phonon transport?

(b) In most applications, 2D materials sit on a substrate or are in contact with a metal electrode. How does the substrate or the electrode material affect phonon transport? This is an important question since the substrate induces additional channels for phonon transport and phonon scattering.

(c) Imperfections such as point defects, vacancies, and grain boundaries inevitably occur in 2D materials. How do imperfections and mechanical strains change the thermal conductivity?

(d) It is rather exciting that 2D materials can be functionalized and intercalated. How can the thermal properties of layered 2D materials be tuned through surface functionalization and intercalation?

We answer these questions in Sec. II from the phonon scattering picture, aiming to give readers a comprehensive physical picture of thermal behavior of 2D materials and its connection with the crystal structures of these materials. Discussions in Sec. II are focused on pristine 2D materials, neglecting defect scattering, boundary scattering, and interface scattering. Since defects and impurities are ubiquitous in real materials, in Sec. III we discuss how defects interfere with phonons and subsequently affect the thermal conductivity. More importantly, surface functionalization and chemical intercalation render an opportunity to tune the thermal conductivity of 2D materials that could enable new functionalities. In Sec. IV, we summarize the main discoveries of current research on phonon and thermal properties of 2D materials, along with the challenges and difficulties in both experimental and theoretical studies. We also suggest some potentially fruitful research directions for 2D materials including electronic thermal transport, topological phonon effect, quantum memory, and sensors.

II. PHONON AND THERMAL PROPERTIES OF PRISTINE 2D MATERIALS

A. Basics of thermal transport in 2D materials

The ability of a solid to conduct heat is characterized by the thermal conductivity κ, which relates a resultant heat flux J to

an applied temperature gradient ∇T via the phenomenological Fourier's law of heat conduction $J = -\kappa \cdot \nabla T$. Depending on the crystal structures, the thermal conductivity can be a scalar in ideally isotropic materials or a tensor in anisotropic materials.

For semiconductors and insulators, heat is mainly carried by phonons, the quantized lattice vibration. According to the kinetic theory (Ziman, 1960; Ashcroft and Mermin, 1978; Chen, 2005), the thermal conductivity in a crystalline material is determined by mode-dependent heat capacity c, group velocity v, and relaxation time τ or mean free path Λ through

$$\kappa = \sum_{\mathbf{q}s} c_{\mathbf{q}s} v_{\mathbf{q}s}^2 \tau_{\mathbf{q}s} = \sum_{\mathbf{q}s} c_{\mathbf{q}s} v_{\mathbf{q}s} \Lambda_{\mathbf{q}s}, \tag{1}$$

where the subscript $\mathbf{q}s$ denotes a phonon mode in the sth phonon branch with a momentum $\hbar\mathbf{q}$ ($\hbar$ is the Planck constant). The mode-dependent heat capacity $c_{\mathbf{q}s}$ is expressed as $\hbar\omega_{\mathbf{q}s}\partial f^0_{\mathbf{q}s}/\partial T$, where $f^0_{\mathbf{q}s} = 1/[\exp(\hbar\omega_{\mathbf{q}s}/k_B T) - 1]$ is the equilibrium phonon population function obeying the Bose-Einstein statistics, $\omega_{\mathbf{q}s}$ is the phonon frequency, and $k_B T$ the product of the Boltzmann constant and the absolute temperature. The phonon dispersion and phonon scattering in this equation can be calculated to reasonably good accuracy by using first-principles-based calculations (Esfarjani, Chen, and Stokes, 2011; Garg *et al.*, 2011; Li, Lindsay *et al.*, 2012). The thermal conductivity can then be determined through the Peierls-Boltzmann transport equation (PBTE) (Broido *et al.*, 2007; Ward *et al.*, 2009; Li, Mingo *et al.*, 2012; Fugallo *et al.*, 2013).

In engineering applications, thermal conductivity is generally regarded as an intensive material property that is independent of sample size. This, however, is valid only when phonon transport is diffusive (Chen, 2001). When the sample size along the transport direction is much smaller than the phonon mean free path $\Lambda_{\mathbf{q}s} (= v_{\mathbf{q}s}\tau_{\mathbf{q}s})$, phonons propagate ballistically across the sample without experiencing appreciable scattering. This is the case in thin films where the thermal conductivity decreases as films become thinner due to the increase of phonon-boundary scattering (Ju and Goodson, 1999). The diffusive phonon transport entails a constant thermal conductivity for sufficiently large samples of 3D materials. However, for some low-dimensional systems, especially in 1D systems (Lepri, Livi, and Politi, 2003; Yang *et al.*, 2012; Chang, 2016), the thermal conductivity does not necessarily converge to a constant value even when the length of a 1D sample is large because there is no scattering mechanism to guarantee diffusive transport.

Even though no rigorous proof is available on whether heat conduction in 2D materials obeys Fourier's law of heat conduction, detailed in Sec. II.B, we adopt the terminology "effective" thermal conductivity used in most literature and compare the heat conducting capability of a few 2D materials, as shown in Fig. 1. The temperature-dependent thermal conductivity values from both the first-principles calculations (Fugallo *et al.*, 2014; Gu and Yang, 2014, 2015; Lindsay *et al.*, 2014; Zhu, Zhang, and Li, 2014; Cepellotti *et al.*, 2015; Jain and McGaughey, 2015; Wang *et al.*, 2015; Peng *et al.*, 2016; Qin and Hu, 2016; Zeraati *et al.*, 2016) and experimental measurements (Cai *et al.*, 2010; Faugeras *et al.*, 2010; Chen *et al.*, 2011, 2012; Lee *et al.*, 2011; Yan *et al.*, 2014; Peimyoo *et al.*, 2015; Zhang *et al.*, 2015), when available, are presented. Experimental measurement of thermal conductivity of 2D materials is still a challenging task. Currently, there are two main techniques to measure the basal-plane (in-plane) thermal conductivity of 2D materials: the optothermal Raman method (Balandin *et al.*, 2008) and the microbridge method (Kim *et al.*, 2001; Shi *et al.*, 2003). The thermal conductivity of 2D materials with sample size around 10 μm long or sufficiently large spans about 3 orders of magnitude from tens of W/mK to thousands of W/mK at room temperature.

In this Colloquium, we tried to correlate the values of thermal conductivity of 2D materials with their crystal structures and atom species. This could not only provide a first-order quantitative estimate on the thermal conductivity value of emerging 2D materials when exact calculations and measurements are not available, but also deepen our understanding of the diverse dependence of the thermal conductivity of many 2D materials on various physical factors.

Indeed, the effort to connect crystal structures and atom species with the macroscopic thermal conductivity of bulk materials can be dated back to the 1970s. Among many models, the Slack equation (Slack, 1973; Morelli and Heremans, 2002)

$$\kappa = A\frac{\bar{M}\theta_a^3 \delta n^{1/3}}{\gamma_G^2 T} \tag{2}$$

is the one used the most. In this equation, n is the number of atoms in the primitive unit cell, δ is the lattice size, θ_a is the Debye temperature of acoustic branches, $\bar{M}$ is the average mass of the atoms in the crystal, γ_G is the Grüneisen parameter, and A is a constant that equals 3.1×10^6 (with the unit of κ in W/mK, $\bar{M}$ in atomic mass unit, T in Kelvin, and δ in Å). The Grüneisen parameter describes the overall effect of the volume change of a crystal on vibrational properties, which is expressed as $\gamma_G = V/C_V(dP/dT)_V$, where V is the volume of a crystal, C_V is the heat capacity at the constant volume, and $(dP/dT)_V$ is the pressure change due to temperature variation at the constant volume. Since the Debye temperature decreases with atomic mass and increases with bonding stiffness, crystals with lighter atomic mass and stronger bonds will have larger $\bar{M}\theta_a^3$ and thus a larger thermal conductivity. On the other hand, with the increase of n, the size of the first Brillouin zone decreases as the volume of the primitive cell increases. Assuming the speed of sound is independent of n, the Debye temperature of the acoustic branches, which is roughly proportional to product of the size of the first Brillouin zone and the sound speed, becomes lower for larger n. As a result, a larger n (number of atoms in the primitive unit cell) leads to a smaller thermal conductivity. Equation (2) has indeed been used as a guideline in searching for high thermal conductivity materials where the requirements are (1) high Debye temperature, (2) small atomic mass, (3) simple crystal structure, and (4) low anharmonicity. Although the Slack equation is derived for 3D materials, these guidelines could be adopted to understand the thermal conductivity of 2D materials. To evaluate the thermal

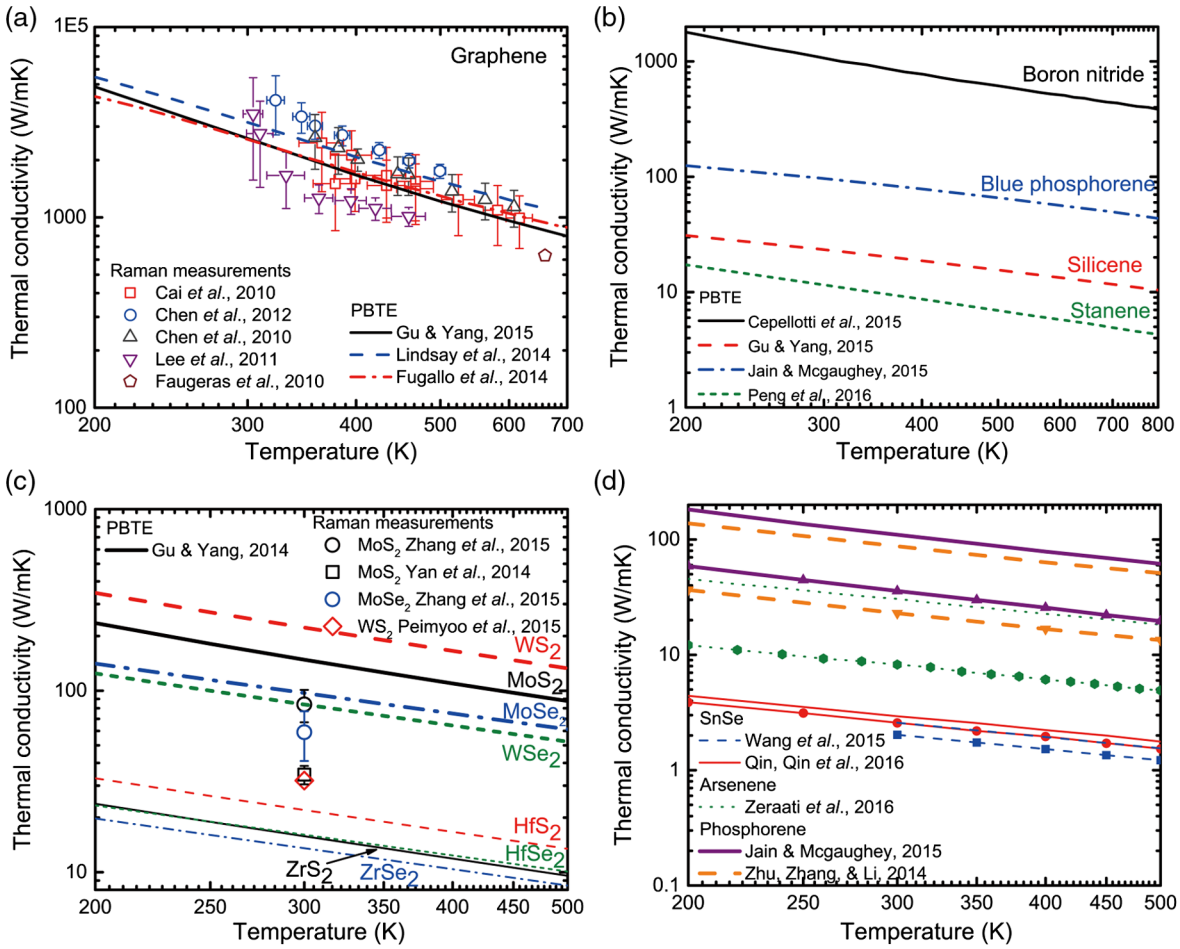

FIG. 1. Thermal conductivities of some typical single-layer 2D materials. (a) Graphene; (b) boron nitride, silicene, stanene, and blue phosphorene, which are of hexagonal crystal structures; (c) a few transition metal dichalcogenides; and (d) a few 2D crystals with puckered structures. The lines in (d) refer the thermal conductivity along the zigzag direction, while the lines with marks are along the armchair direction.

conductivity with Eq. (2), we need to determine the Debye temperature θ_a and the Grüneisen parameter γ_G. Here we first estimate the Debye temperature of the ith acoustic branch, $\theta_{a,i}$ using the group velocity at the Γ point ($\mathbf{q} = 0$), v_i through $\theta_{a,i} = \hbar v_i q_{\text{cut}}/k_B$, with the cutoff wave vector at the zone boundary. Then θ_a is set as the average Debye temperature of the two in-plane acoustic branches $\theta_a = [(1/2)\sum_{i=1,2}\theta_{a,i}^2]^{1/2}$. The Grüneisen parameter γ_G is chosen to be 2.0 here as an estimate for all 2D materials, which was earlier used for graphite by Klemens and Pedraza (1994), although more accurate mode-dependent γ_G can be obtained through first-principles calculations (Mounet and Marzari, 2005). In Fig. 2, we compare the first-principles calculations and the predictions using the Slack equation for the room-temperature thermal conductivity of 2D materials. We see that the Slack equation (2) prediction matches the general trend for thermal conductivity in these known 2D materials. The success of the Slack equation is due to its incorporation of a rough estimate of how all factors in Eq. (1) (i.e., the group velocity, the heat capacity, and the relaxation time) depend on the basic crystal properties. While there are some outliers, such as graphene

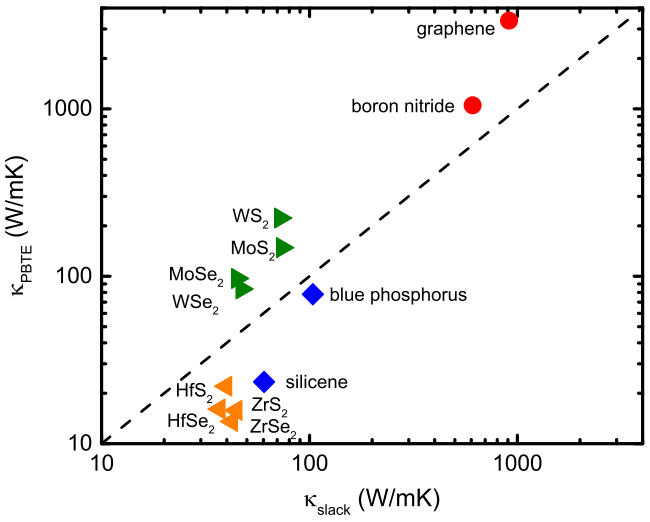

FIG. 2. Comparison of thermal conductivities of some 2D materials calculated from the Slack equation (x axis) and from the first-principles-based PBTE (y axis).

and WS_2, whose thermal conductivity exceeds the predictions of the Slack equation, these deviations could be attributed to the assumption that the Grüneisen constant $\gamma_G = 2.0$ for all the 2D materials instead of varying between materials. In addition, the in-plane modes and flexural out-of-plane modes are not treated independently in the Slack model and the Debye temperature for the flexural out-of-plane acoustic branches is set to zero. As such, the thermal conductivity contributions from the flexural out-of-plane branches are not correctly incorporated in the Slack model.

To gain insight into differences between predictions from the Slack equation and those from the first-principles calculations, Fig. 3 shows the room-temperature thermal conductivity of a few 2D materials, sorted in descending order. Interestingly, the high thermal conductivity materials (such as graphene and boron nitride) have planar structures, the moderate thermal conductivity materials [such as transition metal dichalcogenides (TMDs) whose structure phases are characterized by trigonal prismatic coordination of metal atoms, called 2H TMDs in the literature] have trilayer, mirror symmetric crystal structures, and the low thermal conductivity materials (such as TMDs in their distorted octahedral phases (called 1T TMDs) and buckled materials) have bilayer or trilayer crystal structure without mirror symmetry. This observation reveals that the thermal conductivity of 2D materials is highly sensitive to the crystal structure in addition to the physical factors that are already included in the Slack equation.

To understand the observed correlation between the thermal conductivity and the crystal structure, we first recall the symmetry selection rule in planar 2D materials (Lindsay, Broido, and Mingo, 2010b). If the 2D material is planar, the out-of-plane motion of atoms is completely decoupled from

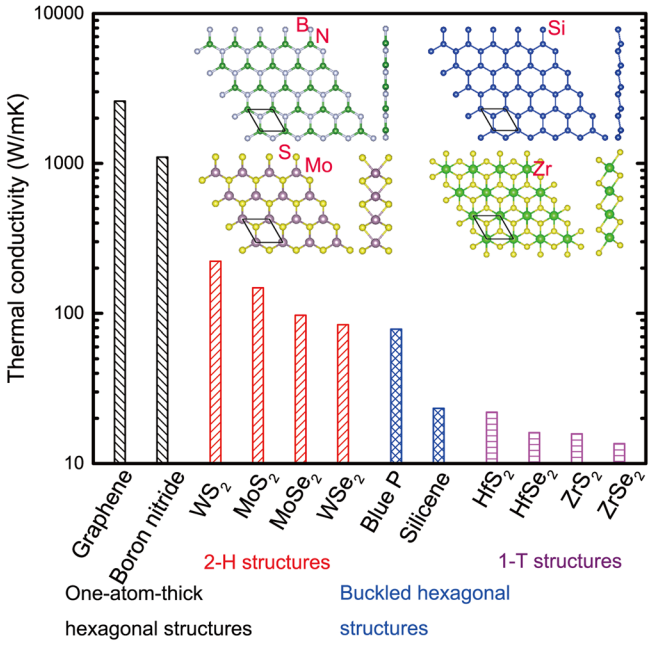

FIG. 3. Thermal conductivity of some typical single-layer 2D materials at room temperature. The data are sorted by descending thermal conductivity values. Inset: The atomic structures of boron nitride, silicene, MoS_2, and ZrS_2 as examples of 2D materials with different crystal structures.

the in-plane motion. As a result, it is possible to classify phonon modes into flexural out-of-plane modes including flexural acoustic (ZA) and flexural optical (ZO) modes, and the in-plane modes including longitudinal acoustic (LA), longitudinal optical (LO), transverse acoustic (TA), and transverse optical (TO) modes. Meanwhile, the planar structure could make the third-order anharmonic force constants $\psi^{\alpha\beta\gamma}_{i,j,k} = \partial^3 E/\partial u^\alpha_i \partial u^\beta_j \partial u^\gamma_k$ zero [the third-order derivative of the total energy of the crystal E with respect to atom displacements including the displacement of atom i (j and k) along direction α (β and γ)], if one or three of the three directions α, β, and γ is the two through-plane directions. This means that simultaneously displacing the three components corresponding to these zero force constants ψ does not lead to anharmonic phonon-phonon scattering. With the three-phonon scatterings involving an odd number of flexural phonon modes, including acoustic (ZA) and optical (ZO) modes, one can easily realize that all third-order force constants are zero by noticing that the atomic motions of flexural modes are purely along the through-plane z direction and those of in-plane modes are purely in the basal plane. Therefore, these three-phonon scattering processes cannot happen (i.e., have a scattering rate of zero), leading to much larger relaxation times for the flexural acoustic phonon modes (Lindsay, Broido, and Mingo, 2010b). This unique selection rule for structures of planar symmetry is one of the main reasons for the large thermal conductivity observed in both the single-layer graphene and boron nitride (Lindsay, Broido, and Mingo, 2010b; Lindsay and Broido, 2011, 2012).

Since 2H TMDs are not planar crystals, the flexural phonon modes are no longer purely out-of-plane vibration. Therefore, the symmetry selection rule breaks down so that the three-phonon scattering processes involving an odd number of flexural phonons are allowed. However, the triplane symmetric structure ensures $\psi^{\alpha\beta\gamma}_{i,j,k}$ to be always equal to zero if i, j, and k denote metal atoms in the middle layer, i.e., that there is no anharmonicity induced by the relative motion of three metal atoms along the z direction. Since the dominant atomic motion of ZA phonons is along the z direction, the scattering rates of these ZA phonon modes are thus very small (Gu, Li, and Yang, 2016). For other 2D crystals, such as buckled honeycomb crystals (Gu and Yang, 2015) and 1T TMDs (Gu and Yang, 2014), there is no symmetry in their crystals which results in stronger phonon scattering compared to planar crystals and 2H TMDs.

Apart from the crystal structure, the atomic masses (atom number) also play an important role in explaining the disparity of thermal conductivity in the group of materials with identical crystal structure. For a few TMDs, the mass of metal atoms is much larger than the chalcogen atoms. A large mass difference of the basis atoms can lead to a large frequency gap between the optical and acoustic phonon branches (Gu and Yang, 2014). For example, the acoustic-optical frequency gap in WS_2 is as large as 110 cm^{-1}, which is close to the range of acoustic phonons of WS_2 (0–178 cm^{-1}), while the gap is only 45 cm^{-1} in MoS_2, much smaller than the frequency range of acoustic phonons (0–230 cm^{-1}). Because of the large phonon frequency gap in WS_2 and the energy conservation requirement of three-phonon scattering, an important phonon scattering

channel [the annihilation process of two acoustic phonon modes into one optical one (acoustic + acoustic → optical)] is strongly suppressed (but not prohibited). As a result, a weaker phonon-phonon scattering rate is observed in WS_2, which yields a much higher thermal conductivity in WS_2 than in MoS_2. While this discussion assumed that three-phonon scatterings were the dominant scattering mechanisms for phonons, recent advances in the theoretical studies have shown that four-phonon scatterings might be important for bulk semiconductors with a large frequency gap, such as boron arsenide, due to the much larger phonon scattering phase space of four-phonon scatterings compared to the three-phonon scatterings (Feng, Lindsay, and Ruan, 2017). We note that the contribution of four-phonon scatterings to phonon transport in 2D materials has not yet been studied. It would be desirable to include four-phonon scatterings, if possible, when studying the thermal transport of 2D materials with large atomic mass difference.

B. The validity of Fourier's law

While thermal conductivity is known to be size independent for 3D materials with large sample size, it remains an open question whether or not the thermal conductivity in 1D and 2D materials is size independent. As summarized in Sec. I, a divergent thermal conductivity scales with sample length L (the positive power exponent ς), $\kappa \sim L^{\varsigma}$ has been observed in most momentum conserving 1D toy lattice models, and also (up to a certain length) in some quasi-1D nanostructures. On the other hand, in the strict 2D systems, as revealed by the Fermi-Pasta-Ulam model, the thermal conductivity scales logarithmically with system size. Recent intensive first-principles calculations for graphene (Fugallo *et al.*, 2014) and graphene nanoribbons (Majee and Aksamija, 2016) indicate that the logarithmic relation seems to hold up to a certain length of ∼1 mm, which is corroborated in experiments using the microbridge measurement (Xu *et al.*, 2014). These first-principles calculations predict that, in order to observe a size independent thermal conductivity, one should utilize samples larger than 1 mm, which is a quite challenging task for experimentalists. In addition, because the crystal structure of graphene is quite different from most other 2D crystals, it is not clear whether the thermal conductivity of these materials shares the same graphene's length dependence.

Figures 4(a) and 4(b) show the experimental setup for thermal conductivity measurements of single-layer graphene with different sample lengths from 300 nm to 10 μm by changing the separation between the heating and sensing membranes, where graphene is suspended on a microbridge device (Xu *et al.*, 2014). Figure 4(c) summarizes the measured thermal conductivity of graphene as a function of sample size (Xu *et al.*, 2014), as well as from calculations including the nonequilibrium molecular dynamics (NEMD) simulations (Park, Lee, and Kim, 2013; Mu *et al.*, 2014; Xu *et al.*, 2014; Barbarino, Melis, and Colombo, 2015) and PBTE calculations (Fugallo *et al.*, 2014; Lindsay *et al.*, 2014; Gu and Yang, 2015; Majee and Aksamija, 2016). NEMD simulations have also been performed to mimic the microdevice based measurement by sandwiching the sample between a hot reservoir and a cold reservoir, where the boundary scattering is

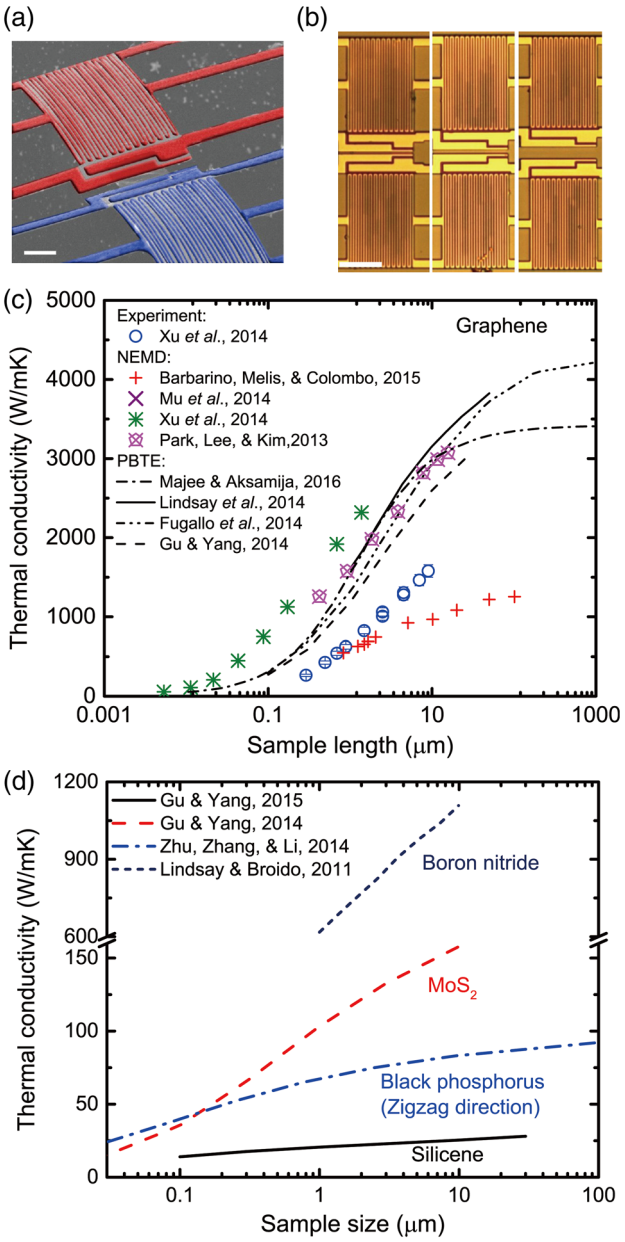

FIG. 4. (a) Scanning electron microscopy image of the microbridge measurement device, which consists of two Pt/SiN_x membranes. The red and blue Pt coils are the heater and temperature sensors, which are thermally connected by suspended graphene (the gray sheet in the middle). Scale bar: 5 mm. (b) SiN_x membrane-based heater structures optimized for length-dependent studies. Scale bar: 20 mm. From Xu *et al.*, 2014. (c) Thermal conductivity of graphene as a function of sample size. (d) Thermal conductivity of some 2D materials as a function of the sample size.

considered in these simulations. For PBTE calculations, a boundary scattering term that is proportional to the ratio between the group velocity of a phonon mode $v_{\mathbf{q}s}$ and sample size L is included, so that phonons are more strongly scattered by the boundaries when the size of the sample is small (Mingo and Broido, 2005). From all of these studies, it is evident that the thermal conductivity of graphene increases with sample size, for room-temperature samples of up to tens of microns.

The thermal conductivity of some other 2D materials from PBTE also exhibits strong length dependence (Lindsay and Broido, 2011; Gu and Yang, 2014, 2015; Zhu and Ertekin, 2014), as shown in Fig. 4(d).

To analyze the thermal conductivity of infinitely large 2D crystals through PBTE, ideally one needs to employ either the iterative approach (Omini and Sparavigna, 1996; Broido, Ward, and Mingo, 2005) or a variational method (Fugallo *et al.*, 2013, 2014). The latter was developed most recently and is equivalent to the iterative approach but numerically more stable and obtains the full solution of the PBTE. The full solution has been shown to be crucial for predicting the phonon transport in 2D materials, such as graphene, where the normal phonon scatterings are stronger than the umklapp scatterings. Unlike the resistive umklapp scatterings, the normal scattering processes do not contribute resistance to heat flow directly, but play important roles in redistributing the nonequilibrium phonon density. When normal scattering dominates, phonon transport deviates from the kinetic picture of a phonon gas obeying the relaxation time (mean free path) approximation, and instead it exhibits hydrodynamic features due to the macroscopic drift motion of phonons (Cepellotti *et al.*, 2015; Lee, Broido *et al.*, 2015). Such a phenomenon can be correctly captured by the full solution of the PBTE. However, since the nonequilibrium phonon population of a specific phonon mode under a temperature gradient is affected by the nonequilibrium population of all other phonon modes in the crystal, the mode-specific thermal conductivity contributed by the phonon modes in the long-wavelength limit cannot be determined unless a computationally infeasible mesh with infinite points is used to sample the first Brillouin zone.

Instead of seeking the full solution of PBTE, we examine the thermal conductivity using Eq. (1). This expression is based on the simple kinetic theory of phonons or equivalently the solution of PBTE under single-mode relaxation time approximation (SMRTA), which uses phonon lifetimes as the phonon relaxation time. The phonon scattering rates for long-wavelength phonons can be determined analytically as discussed later. Comparing to the full solution of PBTE, the SMRTA gives the lower bound value of the thermal conductivity (Fugallo *et al.*, 2013). In other words, we conclude that the thermal conductivity from a more accurate iterative solution of PBTE is unbounded if the thermal conductivity calculation using Eq. (1) under SMRTA is found to be unbounded, but not vice versa. According to Eq. (1), the anomalous thermal conductivity comes from the long-wavelength phonons or acoustic phonons near the Γ point, since the integrand in the equation at other q vectors is a finite number.

Here we focus our discussion on hexagonal 2D crystals, since a large portion of 2D materials possesses such a hexagonal crystal structure. Furthermore, the isotropic phonon dispersion of hexagonal crystals near the Γ point greatly simplifies this analysis. To obtain a finite thermal conductivity of a hexagonal 2D crystal, the long-wavelength (small wave vector) phonons on each phonon branch should satisfy the condition $\omega_{\mathbf{q}s}^2 n_{\mathbf{q}s}^0 (n_{\mathbf{q}s}^0 + 1) v_{\mathbf{q}s}^2 \tau_{\mathbf{q}s}^{\mathrm{ph}} \propto q^n$ with $n > -2$ (Gu and Yang, 2015).

While the in-plane acoustic phonons obey the relationship of $\omega_{\mathrm{TA,LA}} \propto q$ near the Γ point, flexural acoustic phonons strongly depend on the strain conditions in hexagonal 2D materials. According to the elastic theory, the flexural acoustic phonon branch follows $\omega_{\mathrm{ZA}} \propto q^2$ when the sheet is free of stress (Zabel, 2001), which is regarded as a signature of the phonon dispersion curves of 2D materials. However, some complicated theoretical studies predicted that the dispersion deviates from a simple quadratic dependence and is due to mode renormalization (Mariani and von Oppen, 2008; Wang and Daw, 2016). If a 2D material sheet is stretched, even with infinitesimal small strain, the dispersion is linearized, i.e., $\omega_{\mathrm{TA,LA}} \propto q$. Hence, a finite thermal conductivity requires that the relaxation time of a long-wavelength acoustic phonon be $\tau_{\mathbf{q}s}^{\mathrm{ph}} \propto q^n$ with $n > -2$ if the dispersion is linear or $n > -4$ when the dispersion is quadratic.

Recent progress in phonon transport modeling has made it possible to numerically determine the scattering rates for the three-phonon processes (Omini and Sparavigna, 1996; Broido, Ward, and Mingo, 2005; Esfarjani, Chen, and Stokes, 2011) and thus the lifetime of each phonon mode. However, it is still cost prohibitive to numerically distinguish how a phonon lifetime depends on its wave vector as the wavelength approaches zero, since it requires a very fine mesh sampling of the Brillouin zone. Instead, if three-phonon scattering is organized into a series of scattering channels, one can derive analytical expressions for the relation between the wave vector and the scattering rate for each scattering channel (Bonini, Garg, and Marzari, 2012). This provides an efficient approach to find the dominant scattering channels for long-wavelength phonons and thus the dependence of a phonon lifetime with its wavelength.

The scattering of a long-wavelength acoustic mode can be divided into four distinct processes: (1) the annihilation of one phonon mode with another one to generate a third phonon on the same branch, (2) the annihilation of one phonon mode with another one to generate a third phonon on a different branch, (3) the decay of one phonon to two lower-frequency phonon modes on the same branch, and (4) the decay of one phonon to two phonon modes on two lower acoustic branches. These processes are illustrated in Fig. 5. Note that the scaling relation between the scattering rate and the phonon wave vector can vary greatly with strain and crystal structure.

Take unstrained graphene as an example, Bonini, Garg, and Marzari (2012) analytically derived the scattering rates, or the inverse of the phonon lifetimes, for both the in-plane acoustic phonons and the flexural acoustic (ZA) phonons. They found that the long-wavelength in-plane acoustic phonons are predominantly scattered through a decay process that splits one in-plane acoustic phonon into two flexural acoustic phonons due to the quadratic shape of the ZA branch, and the corresponding scattering rate is constant. ZA phonons also scatter with in-plane acoustic phonons in the reverse manner: they are annihilated along with another flexural acoustic phonon to generate a new in-plane acoustic phonon. The scattering rate of ZA modes due to such events scales as q^2, when q approaches zero [see Fig. 6(a)]. Therefore, no matter how phonons are scattered through other scattering channels, the scattering rates of both in-plane acoustic phonons and flexural phonons would satisfy the conditions that ensure a finite thermal conductivity.

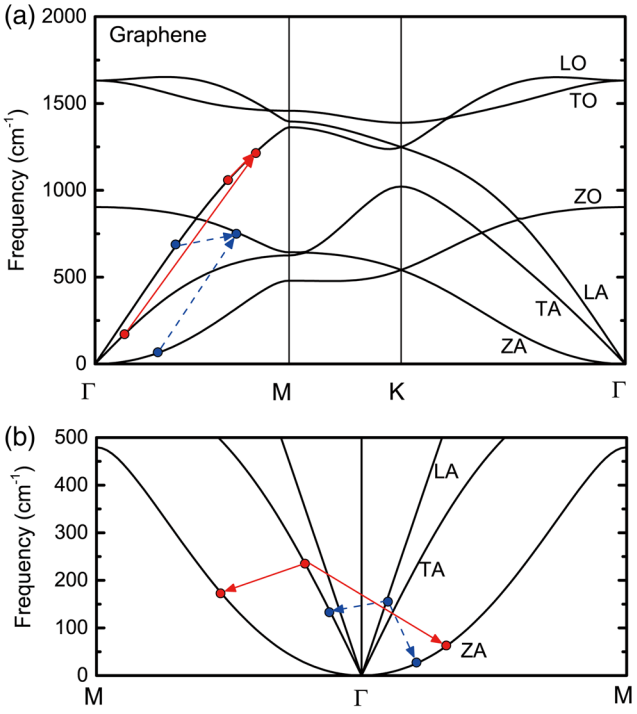

FIG. 5. (a) Schematic representation of phonon annihilation processes using the phonon dispersion curves of single-layer graphene as an example. Solid red arrows: the annihilation of a phonon mode generating a third phonon on the same branch as the second one; dashed blue arrows: the annihilation of a phonon mode generating a third phonon on a different branch from the second one. (b) Phonon decay processes. The solid circles are the phonon modes taking part in the scatterings. The solid circles pointed by arrows are the final states after scattering, while others are the initial states before scattering.

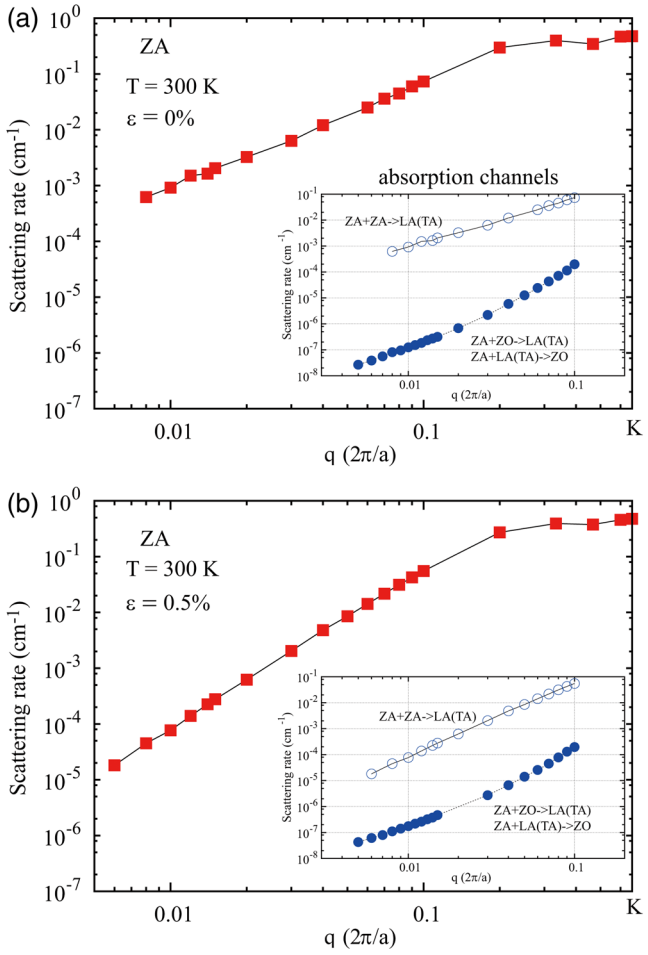

FIG. 6. Scattering rates for the ZA phonon modes along the Γ-K direction in (a) unstrained graphene and (b) graphene under 0.5% tensile strain at 300 K. Inset: Contributions to the total rates ZA + ZA → TA (LA) (open circles) and ZA + ZO → LA (TA) or ZA + LA(TA) → ZO (solid circles). Adapted from Bonini, Garg, and Marzari, 2012.

The equilibrium molecular dynamics (EMD) simulations of Pereira and Donadio (2013) also showed that stress-free graphene has a finite thermal conductivity. They found that the thermal conductivity converges as the size of the simulation domain increases. However, Lindsay (2010) pointed out that the thermal conductivity becomes unbounded when using the iterative solution of PBTE. The underlying mechanisms are still not well understood. Since the main scattering mechanism for a long-wavelength ZA phonon is the normal process in which two ZA phonons annihilate to generate an in-plane acoustic phonon, ZA + ZA ↔ LA/TA (Bonini, Garg, and Marzari, 2012), the unbounded thermal transport could be related to the fact that a large portion of the in-plane phonons is converted to ZA phonons.

When a tensile strain, even an infinitesimal one, is applied to a single-layer graphene, the dispersion of the ZA phonon branch becomes linearized (Bonini, Garg, and Marzari, 2012). In this case, the ZA phonons cannot be as efficiently scattered through the processes where two ZA modes are annihilated into a TA or LA mode (a common process in unstrained graphene), and the scattering rate of long-wavelength ZA phonons scales as q^3 (Bonini, Garg, and Marzari, 2012). Unlike in unstrained graphene, annihilation processes involving ZO phonons become dominant in the long-wavelength limit for strained graphene, whose inverse of scattering rates, or phonon lifetimes, are proportional to q^{-2} [see Fig. 6(b)]. Thus, in the long-wavelength limit, the condition $\tau^{\mathrm{ph}}_{\mathbf{q}s} \propto q^n$ with $n > -2$ does not hold for ZA phonons, and the thermal conductivity of a strained sample diverges logarithmically as the length of the sample increases.

For 2D materials with more than one-atom layer, such as silicene, the symmetry selection rules for the scattering of flexural phonons no longer apply (Gu and Yang, 2015). The scattering of ZA phonons becomes much more frequent than that in the one-atom-thick 2D materials. Numerical calculations showed that the thermal conductivity of infinitely large unstrained silicene, germanene, and stanene sheets has finite values from both a SMRT solution and an iterative solution of PBTE (Y. Kuang *et al.*, 2016).

If the dispersion of a ZA branch is *linear*, the scattering rate of ZA phonons is found to scale as q^{-1} near the Γ point. As a result, the unbounded thermal conductivity does not come from the ZA phonons (as in strained one-atom-thick 2D materials); instead it comes from the long-wavelength LA phonons. According to the analytical derivation of Gu and Yang (2015), only the annihilation process of a

long-wavelength acoustic phonon with two neighboring modes on the same branch could make the inverse of scattering rate follow q^n with $n > -2$. For a long-wavelength LA phonon $\mathbf{q}s$, its frequency can be expressed as $\omega_{\mathbf{q}s} = v_{\mathrm{LA}}q$, with the sound velocity of LA branch v_{LA}. The frequencies of the two phonons $\mathbf{q}'s'$ and $(\mathbf{q}+\mathbf{q}')s''$ on the same branch that can scatter with $\mathbf{q}s$ have to satisfy the condition $\omega_{(\mathbf{q}'+\mathbf{q})s'} - \omega_{\mathbf{q}'s'} = v_{\mathrm{LA}}q$. As q approaches zero, the condition becomes $\mathbf{v}_{\mathbf{q}'s'} \cdot \mathbf{q} = v_{\mathrm{LA}}q$. However, since the sound velocity of the LA branch is usually larger than the group velocity of other phonon modes, long-wavelength LA phonons cannot be scattered by two phonons on the same branch. Thus, the thermal conductivity of silicene with a linear ZA branch diverges, which is not because of the ZA modes but because of the in-plane LA modes. The divergent thermal conductivity of silicene with respect to the sample size was also confirmed by other calculations (Y. D. Kuang *et al.*, 2016; Xie *et al.*, 2016). It is worth mentioning that in the first-principles calculations, due to numerical inaccuracy, the shape of flexural phonons of an unstrained sheet near the Γ point could be linear, which leads to an unbounded thermal conductivity for an infinitely large sheet. By imposing additional invariances on the extracted second-order harmonic force constants from first principles, the quadratic dispersion of flexural phonons can be recovered (Carrete *et al.*, 2016).

It should be noted that this discussion considers only three-phonon scattering processes in hexagonal lattices. Although the higher-order phonon scatterings beyond three-phonon scatterings are usually considered to be weaker than the three-phonon scatterings (Ecsedy and Klemens, 1977), they might play an important role in scattering long-wavelength phonons due to the very large scattering phase space. Given the ultralow bending stiffness of atomic-thin 2D materials (Wei *et al.*, 2013), ripples can easily be formed in those materials under thermal undulation (Fasolino, Los, and Katsnelson, 2007). The ripples could serve as additional channels to scatter phonons. For example, the intrinsic ripples that occur in suspended graphene make the symmetry selection rule break down, leading to stronger phonon scatterings and thus reduces the thermal conductivity. From a rough estimation, one might expect that the corresponding strength enhancement of three-phonon processes is weak (Lindsay, Broido, and Mingo, 2010b), but the additional scattering might alter the scaling relation between the phonon wave vector and the scattering rate for long-wavelength phonons, thus changing the length dependence behavior of the thermal conductivity. While 2D hexagonal crystals have an isotropic dispersion near the Γ point, this is not the case for many other 2D crystal structures. Therefore, the scattering phase spaces of long-wavelength acoustic phonons in nonhexagonal crystals can be quite different from those in hexagonal crystals. For instance, a large portion of long-wavelength LA phonons could scatter with two modes that are on the same branch, as the group velocities of these LA modes are not the largest one among all phonon modes, which is different from hexagonal crystals with a linear ZA branch.

C. Geometrical effects (nanoribbons and few layers)

Width and thickness play an important role not only in determining electronic properties of layered 2D materials, but they can also influence the phonon scattering rate thus altering a material's thermal properties. In conventional materials, when a natural length scale (width, length, or thickness) becomes smaller than the phonon mean free path, the increased phonon-boundary scattering will reduce thermal conductivity. However, when the sample size becomes comparable to the phonon wavelength, phonons are confined to 1D ribbons or 2D planes and the effective thermal conductivity might not decrease monotonically with reduced size. Size-dependent thermal conductivity in 2D crystals could be quite different from that of conventional thin films. In this section, we review recent studies on thermal transport in nanoribbons and few-layer 2D materials and discuss the possible origins of the size dependence.

1. Width dependence

The phonon properties and thermal conductivity of nanoribbons of 2D materials (especially graphene nanoribbons) have been extensively studied, primarily through molecular dynamics (MD) simulations (Guo, Zhang, and Gong, 2009; Hu, Ruan, and Chen, 2009; Evans, Hu, and Keblinski, 2010; Ye *et al.*, 2015; Majee and Aksamija, 2016), PBTE-based simulations (Nika, Ghosh *et al.*, 2009; Nika, Pokatilov *et al.*, 2009; Aksamija and Knezevic, 2011; Nika, Askerov, and Balandin, 2012), and atomistic Green's function (AGF) theory calculations (Xu *et al.*, 2009; Tan, Wang, and Gan, 2011). From most MD and PBTE calculations, the thermal conductivity of graphene nanoribbons is found to be lower than that of larger graphene sheets and it decreases with decreasing ribbon width, although the degree of reduction depends upon the theoretical methods and interatomic potentials employed. The lower thermal conductivity of graphene nanoribbons compared with larger graphene sheets was later confirmed by a few experimental measurements. For instance, thermal conductivity of SiO_2-supported graphene nanoribbons with different lengths and widths was measured using the microbridge method (Bae *et al.*, 2013). The thermal conductivity of single-layer graphene nanoribbons with a length $L = 260$ nm at room temperature was found to increase rapidly with the increase of the nanoribbon width when the width is below 100 nm. Measurements of suspended graphene nanoribbons with submicron length and width were performed using the electrical self-heating method (Xie *et al.*, 2013; Li *et al.*, 2015), where the thermal conductivity of graphene nanoribbons was found to be only several hundred W/mK at room temperature, significantly lower than that of the large suspended graphene sheet.

Despite most work showing that narrow nanoribbons have lower thermal conductivity than wider ones, the AGF calculations show that the normalized thermal conductance (the ratio between thermal conductance and the cross-sectional area of a nanoribbon) decreases with width for many nanoribbons of 2D materials such as graphene (Xu *et al.*, 2009; Tan, Wang, and Gan, 2011), boron nitride (Ouyang *et al.*, 2010), and graphyne (Ouyang *et al.*, 2012). This is due to the harmonic approximation assumed in the atomistic Green's function theory calculations. Atomistic Green's function calculations provide only an upper (ballistic) limit for the thermal conductivity and do not necessarily ensure the correct

width dependence for the thermal conductivity of nanoribbons unless the length of the nanoribbon is much smaller than the phonon mean free path. Indeed, the sample length can also play a role in determining the width-dependent thermal conductivity of nanoribbons (Nika, Askerov, and Balandin, 2012).

Many explanations have been explored to interpret the width-dependent thermal conductivity of graphene nanoribbons. In general, there are three possible explanations: phonon-edge (boundary) scattering, phonon confinement (Tan, Wang, and Gan, 2011), and phonon localization (Wang, Qiu, and Ruan, 2012). In the first explanation, the phonon modes of nanoribbons are assumed to be the bulk phonon modes of a large 2D sheet. These bulk phonons are occasionally scattered by the edges (in addition to the intrinsic phonon-phonon scattering), leading to a lower thermal conductivity than that of a large 2D sheet. The effect becomes more pronounced for a narrower ribbon with rougher edges. Such an explanation has been widely used to explain the lower thermal conductivity of nanostructured bulk semiconductors (Yang and Chen, 2004; Yang, Chen, and Dresselhaus, 2005). In the second explanation, the nanoribbon is treated as a quasi-1D crystal, which has quite different phonon dispersions and scattering rates from those of a large graphene sheet. In particular, the phonon dispersion and group velocities of nanoribbons with different widths differ substantially, resulting in width-dependent thermal transport. In the third explanation, the thermal conductivity reduction of nanoribbons is attributed to phonon localization. The vibration of atoms in the edge is likely to be localized and decoupled from other atoms within the nanoribbon. Localized phonons do not participate in energy transfer.

In addition to the width of nanoribbons, several other factors affecting the thermal conductivity have been identified through numerical simulations, including edge chirality, roughness, and hydrogen passivation. Both MD simulations and AGF calculations showed that a zigzag nanoribbon has a larger thermal conductivity than an armchair nanoribbon of an equal width. According to the phonon-edge scattering interpretation, boundary scattering is expected to be weaker in zigzag nanoribbons because the edge roughness of zigzag nanoribbons is less than that of armchair ones, i.e., the armchair nanoribbon has more edge scatterers per unit length (Haskins *et al.*, 2011). This hypothesis was confirmed by wave-packet MD, where the propagation of phonons is monitored before and after scattering with the edges (Wei, Chen, and Dames, 2012). There were also explanations from the viewpoint of phonon confinement (Xu *et al.*, 2009; Tan, Wang, and Gan, 2011; Ye *et al.*, 2015) and localization (Wang, Qiu, and Ruan, 2012).

Aside from the intrinsic zigzag and armchair edges, the thermal conductivity of nanoribbons could be further reduced by introducing larger scale edge roughness (Evans, Hu, and Keblinski, 2010; Aksamija and Knezevic, 2011; Haskins *et al.*, 2011) or hydrogen passivation (Evans, Hu, and Keblinski, 2010; Hu *et al.*, 2010), which provides additional mechanisms for tuning the thermal conductivity of 2D materials. For example, compared to zigzag nanoribbons of the same width, an introduction of a root mean squared (rms) roughness of 0.73 nm can reduce the thermal conductivity of a 15-nm-wide graphene nanoribbon by 80%. Hydrogen passivation reduces the thermal conductivity by around 50% and 25% for zigzag and armchair graphene nanoribbons with a width of 1.5 nm (Hu *et al.*, 2010), respectively.

While the thermal conductivity of many 2D materials at around room temperature roughly follows a $1/T$ temperature dependence (which is regarded as a sign of strong umklapp phonon-phonon scattering), the thermal conductivity of graphene nanoribbons shows a different trend, where thermal conductivity linearly increases or remains almost unchanged with temperature (Hu, Ruan, and Chen, 2009; Xie *et al.*, 2013). Such temperature dependence should be attributed to the strong phonon-boundary scattering, similar to that in the conventional 3D materials, whose scattering rate is insensitive to temperature. It was recently proposed that at cryogenic temperature (and even up to room temperature) the anomalous thermal conductivity might be due to a second sound (Cepellotti *et al.*, 2015; Lee, Broido *et al.*, 2015), where the effective temperature along the width direction is not uniform but quadratic, just as with the Poiseuille flow velocity profile of fluids in tubes or channels, which is attributed to the fact that normal phonon-phonon scattering processes dominate over resistive umklapp phonon-phonon scattering.

The thermal conductivity of nanoribbons of a few other 2D materials has also been reported, including boron nitride (Sevik *et al.*, 2011) and MoS_2 (Jiang, Park, and Rabczuk, 2013; Liu *et al.*, 2013; T.-H. Liu *et al.*, 2014) using MD simulations. Liu *et al.* (2013) found that the thermal conductivity is almost independent of nanoribbon width. This might be due to the strong anharmonicity in the empirical potentials employed in their MD simulations. It should always be kept in mind that the calculated thermal conductivity depends strongly on the empirical potentials employed when interpreting the MD results.

Because of the low thermal conductivity of nanoribbons, the thermoelectric performance of nanoribbons of many materials has also been studied. Different strategies have been proposed to further suppress the thermal conductivity while maintaining good electronic transport (Nguyen *et al.*, 2014; Hossain *et al.*, 2015; Tran *et al.*, 2017), for example, introducing defects in nanoribbons and constructing junctions of two different 2D materials.

2. Layer thickness dependence

The thermal conductivity of thin films of a few layered 2D materials, such as black phosphorus (Jang *et al.*, 2015; Lee, Yang *et al.*, 2015; Luo *et al.*, 2015; J. Zhu *et al.*, 2016), $TaSe_2$ (Yan *et al.*, 2013), and Bi_2Te_3 (Pettes *et al.*, 2013), with a thickness on the order of 10 to 100 nm, has been measured. The thermal conductivity of these layered 2D materials was reported either to be substantially lower than that of their bulk counterparts or to increase with sample thickness. This observation seems to support the argument that the classic size effects in conventional 3D materials, which assumes that boundary scattering reduces the thermal conductivity, also occur in layered 2D crystals. However, when the thickness is further reduced to around 10 nm, the dependence of thermal conductivity on sample thickness becomes quite complicated, likely due to the change of phonon dispersion. While Raman

spectra of a variety of few-layer 2D materials have provided the evidence of thickness-dependent phonon properties (Ferrari *et al.*, 2006; H. Li *et al.*, 2012; Castellanos-Gomez *et al.*, 2014), the thickness dependence of thermal conductivity in these materials is not conclusive yet due to the possible change of both phonon dispersion and phonon scattering. Here we present a summary of these studies on thickness-dependent thermal conductivity of some layered 2D materials, including graphene, MoS_2, Bi_2Te_3, and black phosphorus.

Figure 7(a) shows the thermal conductivity of graphite, few-layer graphene, and single-layer graphene. The thermal conductivity of graphite is measured to be about 2000 W/mK at room temperature, while that of single-layer graphene ranges from 2500 to 5000 W/mK. The theoretical studies using both NEMD (Z. Wei *et al.*, 2011) and PBTE (Lindsay, Broido, and Mingo, 2011; Singh, Murthy, and Fisher, 2011; Kuang, Lindsay, and Huang, 2015) confirmed that single-layer graphene has a much higher thermal conductivity than that of graphite. As discussed in Sec. II.A, this is because phonon scattering in single-layer graphene has to obey the symmetry selection rule (Lindsay, Broido, and Mingo, 2010b), which leads to a smaller scattering phase space and weaker scattering for the flexural (ZA) phonon modes. Some experiments (Ghosh *et al.*, 2010) and most of the numerical simulations (Lindsay, Broido, and Mingo, 2011; Singh, Murthy, and Fisher, 2011; Kuang, Lindsay, and Huang, 2015) further showed that thermal conductivity gradually decreases when the number of layers is increased, while some other experiments reported much smaller thermal conductivity (Pettes *et al.*, 2011) due to polymer residues on the samples. In encased graphene, the inverse thickness dependence of the thermal conductivity has been observed (Jang *et al.*, 2013).

Theoretical studies (Yan, Ruan, and Chou, 2008; Lindsay, Broido, and Mingo, 2011) showed that additional ZA-like low-frequency optical phonon branches are generated in multilayer graphene. Compared to the ZA modes in single-layer graphene, these ZA-like phonons in multilayer graphene have lower average phonon group velocities and much larger phonon scattering rates due to the greater number of scattering channels available, which results in a lower thermal conductivity. A similar monotonic reduction of thermal conductivity with respect to the number of layers was also reported for graphene nanoribbons from MD simulations (Zhong *et al.*,

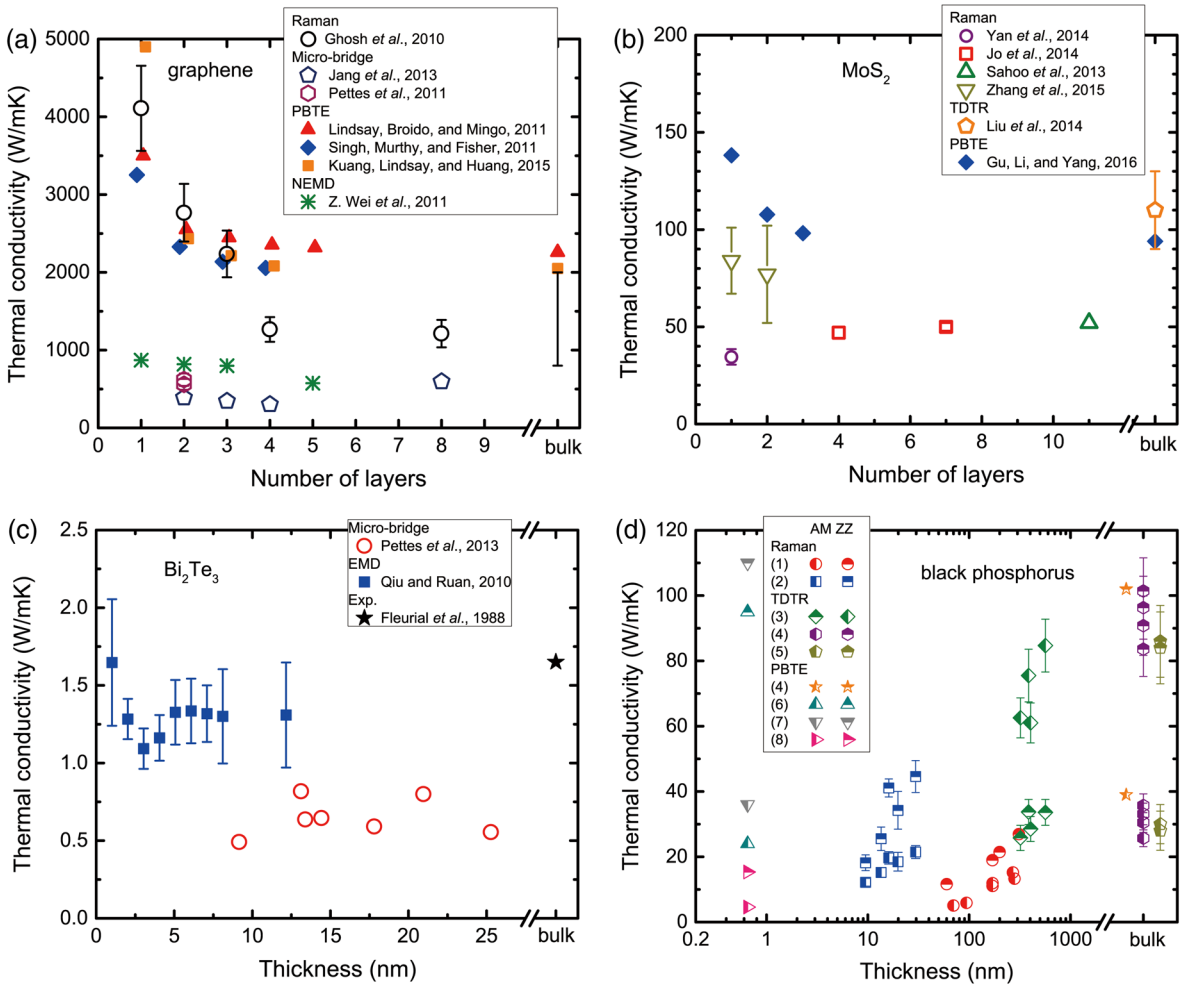

FIG. 7. Thickness-dependent thermal conductivity of (a) graphene, (b) MoS_2, (c) Bi_2Te_3, and (d) black phosphorus. The data in (d) come from (1) Lee, Yang *et al.* (2015), (2) Luo *et al.* (2015), (3) Jang *et al.* (2015), (4) J. Zhu *et al.* (2016), (5) Sun *et al.* (2017), (6) Zhu, Zhang, and Li (2014), (7) Jain and McGaughey (2015), and (8) Qin, Zhang *et al.* (2016). The layer coordinates for some data in (a) and (d) have been offset slightly for clarity.

TABLE I. Experimental studies on the thermal conductivity of MoS_2. χ is the temperature coefficient of the Raman signal and α is the absorption ratio used for data fitting. Adapted from Gu, Li, and Yang, 2016.

Ref.	Method	Sample type	Room-temperature thermal conductivity (W/mK)	Experimental conditions
Yan *et al.* (2014)	Raman	Exfoliated, transferred	34.5 ± 4 (1 layer)	A_{1g} mode, $\chi = 0.011$ cm^{-1}/K, $\alpha = 9\% \pm 1\%$, 170-nm-diameter laser spot, suspended on 1.2-μm-diameter holes, ambient condition
Zhang *et al.* (2015)	Raman	Exfoliated, transferred	84 ± 17 (1 layer)	A_{1g} mode, $\chi = 0.0203$ cm^{-1}/K, $\alpha = 5.2\% \pm 0.1\%$, 460–620-nm-diameter laser spot, suspended on 2.5-to-5.0-μm-diameter holes, ambient condition
Zhang *et al.* (2015)	Raman	Exfoliated, transferred	77 ± 25 (2 layer)	A_{1g} mode, $\chi = 0.0136$ cm^{-1}/K, $\alpha = 11.5\% \pm 0.1\%$, 460–620-nm-diameter laser spot, suspended on 2.5-to-5.0-μm-diameter holes, ambient condition
Jo *et al.* (2014)	Microbridge	Exfoliated, transferred	44–50 (4 layer)	Suspended sample; length: 3 μm, width: 5.2 μm.
Jo *et al.* (2014)	Microbridge	Exfoliated, transferred	48–52 (7 layer)	Suspended sample; length: 8 μm, width: 2.2 μm.
Sahoo *et al.* (2013)	Raman	Chemical vapor deposition, transferred	52 (11 layer)	A_{1g} mode, $\chi = 1.23 \times 10^{-2}$ cm/K, $\alpha = 10\%$, 1–1.5 μm laser spot, suspended on a 10-μm-radius quadrant, ambient condition
Liu, Choi, and Cahill (2014)	Pump probe	Bulk	85–112	Modulation frequency of pump beam: 10.7 MHz

2011; Cao *et al.*, 2012) and boron nitride from PBTE-based calculations (Lindsay and Broido, 2012), which could be explained by the similar reasons revealed for graphene.

Compared to graphene, recent experiments showed a quite different trend for the layer thickness-dependent thermal conductivity of MoS_2, as summarized in Fig. 7(b) and Table I. While the measured basal-plane thermal conductivity of single-layer MoS_2 by different researchers differs, due to differences in sample quality and experimental conditions, the thermal conductivity of MoS_2 with more than four layers seems to follow an opposite trend from that of graphene, i.e., the thermal conductivity of MoS_2 increases with the number of layers. A recent first-principles-based PBTE study (Gu, Li, and Yang, 2016) showed that the basal-plane thermal conductivity of 10-μm-long samples reduces monotonically from 138 to 98 W/mK for naturally occurring MoS_2 when its thickness increases from one layer to three layers, and the thermal conductivity of trilayer MoS_2 approaches that of bulk MoS_2. The reduction is attributed to both the change of phonon dispersion and the thickness-induced anharmonicity. Phonon scattering for ZA modes in bilayer MoS_2 is found to be substantially larger than that of single-layer MoS_2, which is attributed to the fact that the additional layer breaks the mirror symmetry as discussed in Sec. II.A. In Fig. 7(b), the measured thermal conductivity of MoS_2 is also presented (Sahoo *et al.*, 2013; Jo *et al.*, 2014; Liu, Choi, and Cahill, 2014; Yan *et al.*, 2014; Zhang *et al.*, 2015), but the experimental results show no clear thickness dependence.

Bi_2Te_3 is another interesting layered 2D material, which has been widely studied in the fields of thermoelectrics (Venkatasubramanian *et al.*, 2001; Poudel *et al.*, 2008) and topological insulators (Y. Chen *et al.*, 2009; Zhang *et al.*, 2009). As shown in Fig. 7(c), an EMD study (Qiu and Ruan, 2010) on few-layer Bi_2Te_3 showed that the thermal conductivity of Bi_2Te_3 does not change monotonically with thickness, but exhibits a minimum at a thickness of three quintuples. At a thickness of 5 nm (five quintuples), the thermal conductivity recovers to that of the bulk counterpart. Such a nonmonotonic layer thickness dependence was attributed to the competition between phonon-boundary scattering and the umklapp phonon-phonon scattering in the thickness range they explored (Qiu and Ruan, 2010). However, such a theoretical prediction seems to conflict with the microbridge measurement for Bi_2Te_3 thin films of 9 to 25 nm thickness (Pettes *et al.*, 2013). Pettes showed that the thermal conductivity roughly increases with thickness. Note that the experimental measurements by Pettes are on much thicker samples, while the calculation by Qiu and Ruan (2010) are for thin samples with only a few layers.

Figure 7(d) shows the measured thermal conductivity of black phosphorus along both the zigzag and the armchair directions from different research groups (Jang *et al.*, 2015; Lee, Yang *et al.*, 2015; Luo *et al.*, 2015; J. Zhu *et al.*, 2016; Sun *et al.*, 2017). Interestingly, in both directions the measured thermal conductivity of black phosphorus thin films increases with the thickness, although the data from different groups vary noticeably. While the PBTE prediction for bulk black phosphorus agrees well with time-domain thermoreflectance measurements, there is still a large discrepancy among the predicted thermal conductivities of single-layer black phosphorene (Zhu and Ertekin, 2014; Jain and McGaughey, 2015; Qin, Zhang *et al.*, 2016), due to the choice of the cutoff of interatomic forces and whether the van der Waals interaction is considered in the first-principles calculations (Qin, Zhang *et al.*, 2016).

From this summary on the thickness-dependent thermal conductivity of several layered 2D materials, it can be seen that there is a large gap between the theoretically calculated results and the experimental measurements. The calculated

thermal conductivity of 2D materials with one or few layers is usually higher than that of the bulk counterpart, while the measurement usually does not follow such a trend. Polymer residues, absorbed gas, and oxidization are considered to contribute to this discrepancy. To better understand the difference between the theoretical calculations and measured data, more efforts on numerical simulations should be given to the study of thermal properties of more realistic materials in order to see how imperfections, which are common in experiments, affect the thermal conductivity of 2D materials.

Apart from stacking 2D layers based on their bulk forms, for example, *AB* stacking for graphene and MoS_2, it is possible to stack different layers in other ways to achieve few-layer pristine 2D materials with novel thermal properties. Nika, Cocemasov, and Balandin (2014) and Cocemasov, Nika, and Balandin (2015) theoretically studied the phonon properties and the in-plane thermal conductivity of twisted bilayer graphene. The Raman-based optothermal measurement confirmed that the thermal conductivity of such bilayer graphene could be substantially lower than that of the bilayer graphene with *AB* stacking (Li *et al.*, 2014). Stacking the exfoliated Bi_2Te_3 thin films to form the "pseudosuperlattice" has been proven as an effective method to reduce the thermal conductivity from the bulk value (Goyal, Teweldebrhan, and Balandin, 2010; Teweldebrhan, Goyal, and Balandin, 2010). The thermal conductivity reduction is thought to be due to the rough boundary scattering or spatial confinement effect of acoustic phonons (Teweldebrhan, Goyal, and Balandin, 2010).

D. Strain effects

Strain and deformation commonly exist in 2D materials. When 2D materials are integrated into nanodevices, typically they are deformed due to constraints imposed during device assembly. When two or more kinds of 2D crystals are vertically stacked or laterally connected to form heterostructures, 2D materials are likely to be strained due to the lattice mismatch. On the other hand, strain engineering has also been proposed to tune electronic, photonic, and even thermal properties (Mohiuddin *et al.*, 2009; Conley *et al.*, 2013; Fan *et al.*, 2017).

The studies on strain-dependent thermal conductivity of solids and liquids can be traced back to the 1970s and 1980s (Ross *et al.*, 1984), where strain was usually induced by pressure (compressive stress). The experimental demonstration of utilizing strain to actively control phonon and thermal properties has been applied to many different kinds of material systems (Hsieh *et al.*, 2009, 2011; Alam *et al.*, 2015). Theoretical studies have also been performed to understand the origins of strain-dependent thermal conductivity of both bulk crystals (Picu, Borca-Tasciuc, and Pavel, 2003; Bhowmick and Shenoy, 2006; Li *et al.*, 2010; Parrish *et al.*, 2014) and nanostructured materials (Xu and Li, 2009; Xu and Buehler, 2009; Li *et al.*, 2010). While it is necessary to quantify the strain dependence of thermal conductivity, it is still more challenging to precisely control the exerted strain in 2D materials than in 3D materials. Therefore, the study of strain-dependent thermal conductivity of many 2D materials has been limited to just numerical simulations.

Li *et al.* (2010) conducted EMD simulations to show that the thermal conductivity of graphene monotonically decreases with the increase of tensile strain, similar to most bulk materials. However, the calculations of Fan *et al.* (2017) using both EMD and NEMD showed an increase in thermal conductivity with the increase of tensile strain, particularly due to the contributions from flexural modes. Recent calculations using PBTE-based approaches give quite different trends for strain dependence. For example, under RTA Bonini, Garg, and Marzari (2012) found that the thermal conductivity of strained graphene is unbounded, due to the weak scattering for ZA phonons, and the tensile strain enhances the thermal conductivity in the strain range they explored for an infinite large graphene sheet. Some other researchers (Fugallo *et al.*, 2014) showed that the thermal conductivity of graphene is a finite value when the PBTE is solved iteratively. The tensile strain is also found to either enhance or reduce the thermal conductivity of graphene depending on the sample size (Fugallo *et al.*, 2014; Y. Kuang *et al.*, 2016). Many of these discrepancies indeed come from computational details. In MD simulations, due to the finite simulation domain size, the phonons whose wavelengths are larger than twice the simulation domain size do not exist in the simulation system and thus do not contribute to the thermal conductivity. As the long-wavelength phonons play unique roles in 2D crystals (as discussed in Sec. II.B), the thermal conductivity results from MD simulations could be sensitive to both the size of the simulation domain and the treatments employed to compensate for the thermal conductivity from the long-wavelength phonons. For PBTE calculations, a finite number of $\mathbf{q}$ points are used for numerical integration over the Brillouin zone where the heat conducted by long-wavelength phonon modes near the first Brillouin zone center is not counted and the calculated thermal conductivity exhibits a strong q-mesh dependence, just like the simulation domain size effects in MD simulations. The strain dependence on thermal conductivity from PBTE calculations might not be justified if the calculations are performed using a $\mathbf{q}$ mesh with a fixed number of $\mathbf{q}$ points. Special attention needs to be paid to the computational details when interpreting these simulation results.

Figure 8(a) shows that the strain dependence of thermal conductivity in other single-layer 2D materials is quite diverse. A monotonical reduction of thermal conductivity was observed for single-layer MoS_2 from MD simulations (Jiang, Park, and Rabczuk, 2013) and for pentagraphene from PBTE (Liu *et al.*, 2016). The thermal conductivity of some buckled 2D crystals, e.g., silicene (Y. D. Kuang *et al.*, 2016; Xie *et al.*, 2016) and penta-SiC_2 (Liu *et al.*, 2016), and few-layer 2D materials, such as graphene and boron nitride (Kuang, Lindsay, and Huang, 2015), exhibits a nonmonotonic (up-and-down) relation with strain. Penta-SiN_2 was discovered from a first-principles-based PBTE calculation to have a very unusual thermal conductivity dependence on strain, which is increased by an order of magnitude at a tensile strain of 9% (Liu *et al.*, 2016).

The diverse dependence of thermal conductivity on strain for different 2D materials can be attributed to the different strain dependence of heat capacity, group velocity, and phonon-phonon scattering rates for 2D sheets with different crystal structures in accordance with the simple kinetic theory.

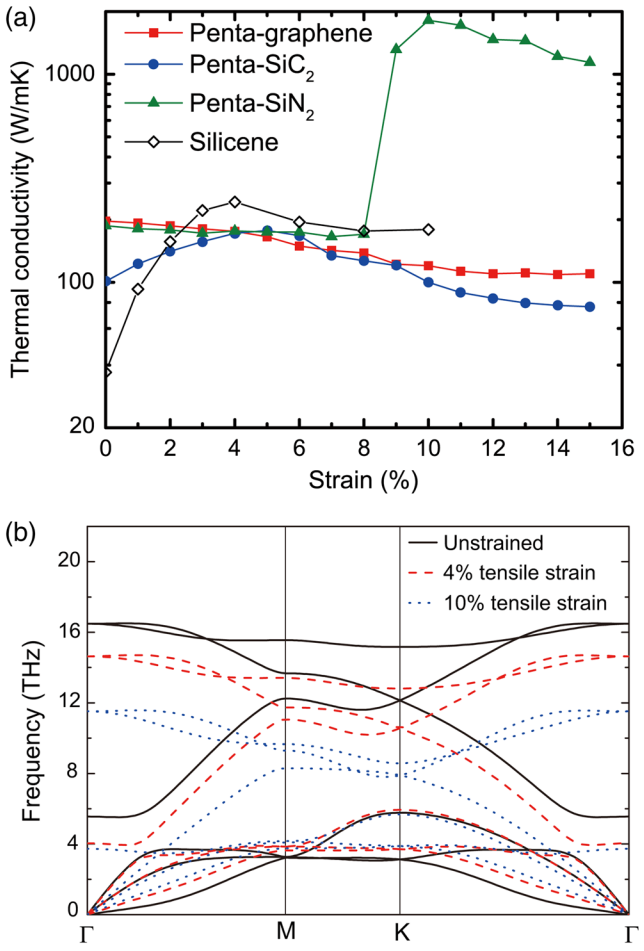

FIG. 8. (a) Thermal conductivity of some 2D materials as a function of tensile strain. (b) Phonon dispersion of silicene under different tensile strain. From Xie *et al.*, 2016.

In general, the stretching of a material could lead to a downshift of the phonon spectra for many 3D materials. This is also true for most 2D materials. Figure 8(b) shows phonon dispersion of silicene as an example (Xie *et al.*, 2016). In most of the calculated phonon dispersions of tensile stained 2D materials, we observe optical phonon softening (Liu, Ming, and Li, 2007; Li, 2012; Xie *et al.*, 2016). For acoustic phonons, the frequency of the longitudinal and transverse acoustic phonons shows a similar reduction, but the flexural acoustic phonons behave differently near the Γ point due to phonon stiffening. Therefore, tensile strain could either increase or reduce the phonon group velocities. When the strain is large, the downshift of phonon spectra might be significant and the velocity of most phonon modes is thus reduced.

Apart from the phonon dispersion, lattice distortion (including phase change) could be another reason for the diverse responses of thermal conductivity when a tensile strain is applied. For many non-one-layer-thick 2D crystals, such as those with buckled structure, tensile strain could substantially reduce the buckled distance, e.g., silicene (Xie *et al.*, 2016), or even eliminate the buckling, e.g., penta-SiN_2 (Liu *et al.*, 2016). As discussed in Sec. II.B, the buckled structure could induce strong scattering for ZA phonons (as well as LA and TA phonons). Thus, applying tensile strain weakens phonon scattering by partially recovering the selection rule of symmetry. The interplay between the shift of phonon spectra and the change of phonon scattering channels results in the nonmonotonic strain dependence of thermal conductivity for many 2D materials.

For example, the up-and-down strain-dependent thermal conductivity for silicene was observed from PBTE calculations (Y. D. Kuang *et al.*, 2016; Xie *et al.*, 2016); see Fig. 8(a). The thermal conductivity increased first to about 8 times the unstrained state's at 4%–8% tensile strain, then it decreased by around 10%–50% the maximum thermal conductivity when the tensile strain was further increased to 10%. When tensile strain is applied, the strain-induced flattening of the structure weakens many of the dominant scattering channels in unstrained silicene, such as $ZA + ZA \rightarrow ZA$, $ZA \rightarrow ZA + ZA$, or $TA + ZA \rightarrow LA/TA$, resulting in an increased thermal conductivity. These suppressed channels correspond to totally forbidden channels in the purely planar 2D crystals (e.g., graphene). The sudden jump of thermal conductivity of 2D penta-SiN_2 at an 8% strain, shown in Fig. 8(a), is due to the transition of penta-SiN_2 from a buckled lattice to a flat one.

Compressive strain also greatly affects the thermal conductivity of 2D crystals. According to EMD simulations (Li *et al.*, 2010), an 8% compressive strain reduces the thermal conductivity of graphene by 50% relative to its unstrained state. The decrease of thermal conductivity with respect to compressive strain is attributed to compression induced rippling of graphene, since rippling could induce additional phonon scattering channels in addition to the intrinsic phonon-phonon scattering. Similar compressive strain dependence of thermal conductivity is observed in other MD simulations (Guo, Zhang, and Gong, 2009; N. Wei *et al.*, 2011). Lindsay, Broido, and Mingo (2010a) studied the thermal conductivity of carbon nanotubes with different diameters using the Boltzmann transport equation and showed that the thermal conductivity of graphene is larger than that of carbon nanotubes with different diameters due to the breakdown of symmetry selection rules in carbon nanotubes. Although phonon transport in carbon nanotubes is not exactly the same as rippled graphene, this theoretical study explicitly shows that the thermal conductivity is highly affected by the curvature of 2D sheets. Compared with graphene, studies on other 2D materials are relatively scarce, except a very limited few based on MD simulations; see, e.g., Ding *et al.* (2015).

E. Device geometry (effect of substrates)

When 2D materials are integrated for device applications, the heat dissipation channels and thermal properties of 2D materials change dramatically from the suspended ones due to their contact with a substrate. While the heat generated in a suspended 2D material has to flow within the suspended sample and then dissipate to the substrate at the contact regions, in a device geometry heat could simultaneously flow in the sample and dissipate to the substrate directly by penetrating across the interfaces between 2D material and the substrate. Therefore, for a good understanding of heat dissipation in devices it is crucial to know both the thermal conductivity of supported 2D material and the interfacial thermal conductance between 2D materials and substrates. In this section, we first

discuss the change of thermal conductivity of 2D materials when they are supported, followed by the interfacial thermal conductance between 2D material and substrates.

1. Thermal conductivity of supported 2D materials

The basal-plane thermal conductivity of a supported 2D crystal is very different from a suspended one, even though in most cases the interaction between the 2D materials and the substrates is weak (typically is of van der Waals type). Pioneering work on the effect of substrates on phonon transport in 2D materials was done by Seol *et al.* (2010), where the thermal conductivity of supported graphene on silicon dioxide substrate was measured using the microbridge method. The measured thermal conductivity is only around 600 W/mK as shown in Fig. 9(a). This is very close to the value predicted by NEMD simulations (Chen, Zhang, and Li, 2013), where monolayer graphene is placed on top of a SiO_2 substrate. The thermal conductivity of graphene on a SiN_x substrate was systematically studied by Wang (2013) and was found to be only around 430–450 W/mK. As the number of 2D material layers increases, the thermal conductivity increases as shown in Fig. 9(b). Other experimental measurements, including those using the optothermal Raman method (Cai *et al.*, 2010), the 3-ω heat spreader (Jang *et al.*, 2013), and the frequency domain thermoreflectance measurement (Yang *et al.*, 2014), also confirmed thermal conductivity reduction of graphene when it is placed on top of a silicon oxide substrate or sandwiched between two substrates. Taube *et al.* (2015) measured the supported 2D MoS_2 using the optothermal Raman method and showed a lower thermal conductivity value when compared with that of suspended samples.

Substrates affect the thermal conductivity of supported samples in two distinct ways: changing the phonon dispersion and enhancing the phonon scattering rate. Raman spectra measurements provide direct evidence for substrate effects on optical phonons (Berciaud *et al.*, 2009). Many theoretical studies were devoted to deepening the understanding of phonon transport in supported 2D materials. The phonon-substrate scattering rates have been derived using the scattering matrix method, where the effects of substrate are modeled as point defects to the 2D crystal (Seol *et al.*, 2010). Under a harmonic approximation and assuming that the phonon dispersion of the supported graphene is identical to the freestanding one, Seol *et al.* found that phonon scattering increases with the enhancement of the averaged van der Waals interatomic force constant between the graphene and the SiO_2 support. This model qualitatively explains the thermal conductivity reduction of supported graphene. A few MD simulations were performed to predict the thermal conductivity of supported 2D materials (Ong and Pop, 2011; Chen and Kumar, 2012; Qiu and Ruan, 2012; Chen, Zhang, and Li, 2013; Wei, Yang, Bi, and Chen, 2014). Spectral energy density analysis shows that the relaxation time of acoustic phonons is reduced more pronouncedly than that of optical phonons when graphene is placed on top of a silicon oxide substrate, and the flexural acoustic (ZA) phonons are most affected (Qiu and Ruan, 2012). Because of the renormalization of ZA phonons, the frequency of the ZA phonon is no longer zero at the Γ point, but is a finite value and the scattering of ZA phonons is enhanced (Ong and Pop, 2011). The shift of phonon dispersion also contributes to the interesting length dependence of the thermal conductivity in graphene. As predicted by NEMD simulations (Chen, Zhang, and Li, 2013), the thermal conductivity of supported graphene is almost unchanged when the length is larger than 100 nm whereas in suspended graphene it increases even when the length is larger than 1 μm. Chen, Chen, and Gao (2016) studied thermal conductivity of supported black phosphorus using NEMD simulations and found that the degree of anisotropy becomes larger when supported.

Intuitively, a stronger coupling of 2D crystals to the substrate would lead to a larger reduction in thermal

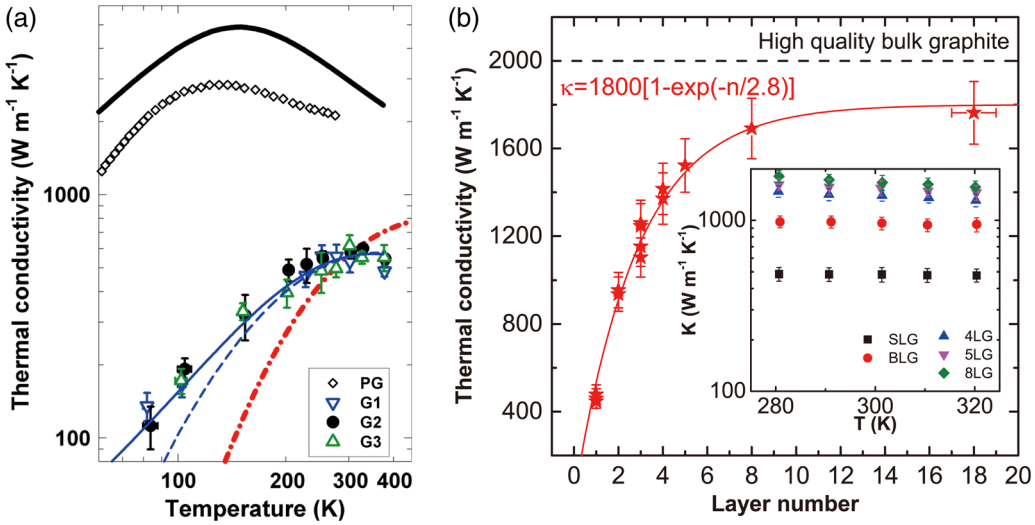

FIG. 9. (a) Measured thermal conductivity of supported graphene (on SiO_2) together with the highest reported values of pyrolytic graphite (PG). G1, G2, and G3 refer to the three graphene samples. From Seol *et al.*, 2010. (b) Measured room-temperature thermal conductivity of supported graphene (on SiN_x) as a function of the number of atomic layers (red star) with the best-fit curve (red line). Inset: Temperature dependence of thermal conductivity around 300 K. From Wang, 2013.

conductivity, since the vibration of 2D materials would be more severely affected, as indicated by the phonon-substrate scattering rates derived using the scattering matrix method (Seol *et al.*, 2010). Most MD simulations confirmed such a relationship between the coupling strength and the thermal conductivity for supported graphene (Chen and Kumar, 2012; Qiu and Ruan, 2012; Chen, Zhang, and Li, 2013; Wei, Yang, Bi, and Chen, 2014). Some MD simulations, however, showed that this is not necessarily true. For example, Ong and Pop (2011) found that when the strength of graphene-substrate interaction is increased by 2 orders of magnitude, heat flow along supported graphene (or equivalently its thermal conductivity) increases by up to 3 times. They found that the strong coupling between quadratic ZA modes of graphene and the surface waves of the substrate leads to a hybridized linear dispersion with a reduced scattering rate and higher phonon group velocity.

The thermal conductivity of supported 2D materials depends not only on the substrate coupling strength previously described, but also on the nature of substrates. A recent study by Zhang *et al.* (2017) found that a substrate such as *h*-BN (which has a very similar structure to graphene) does not significantly reduce the thermal conductivity of graphene.

Since the thermal conductivity of most 2D materials is suppressed when they are weakly bonded to a substrate, it is desirable to identify the thickness (layer number) beyond which the thermal conductivity of layered 2D material thin films recovers to the freestanding sample's higher value. Figure 10 shows the layer thickness-dependent thermal conductivity of both supported and encased few-layer graphene. In both measurements (Jang *et al.*, 2013; Sadeghi, Jo, and Shi, 2013; Yang *et al.*, 2014) and NEMD simulations (Chen, Zhang, and Li, 2013), the thermal conductivity is found to increase with the number of atomic layers, in contrast to the suspended graphene where the thermal conductivity decreases with the layer number. Encased ten-layer graphene has a thermal conductivity larger than 1000 W/mK (Jang *et al.*, 2013), and the supported graphene of 34 layers is found to fully recover to the bulk value of graphite (Sadeghi, Jo, and Shi, 2013). The large thickness required to ensure a higher thermal conductivity of encased and supported graphene is probably due to the long mean free paths of phonons in graphite along the cross-plane direction, which was revealed recently by MD simulations (Wei, Yang, Chen *et al.*, 2014) and confirmed by experimental measurements (Fu *et al.*, 2015; Zhang *et al.*, 2016).

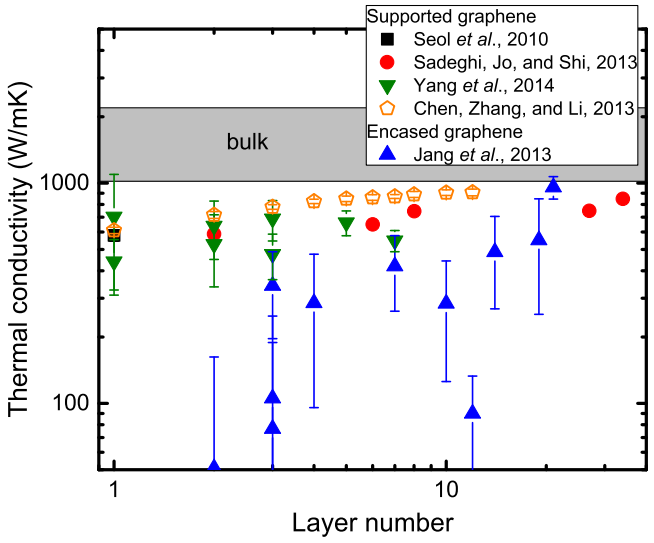

FIG. 10. Thermal conductivity of supported or encased few-layer graphene at room temperature as a function of sample thickness.

2. Interfacial thermal conductance between 2D materials and substrates

Heat flows across the interfaces between 2D materials and substrates and subsequently dissipates to the substrates. The interfacial thermal conductance between graphene or graphite and a wide range of substrates has been studied. The typical values of the interfacial thermal conductance between graphene and substrate materials, such as SiO_2, aluminum, and gold thin film, range from 20 to 100 MW/m^2K at room temperature and have been summarized in a few articles (Sadeghi, Pettes, and Shi, 2012; Ni, Chalopin, and Volz, 2013; Xu, Li, and Duan, 2014). Several groups have measured the interfacial thermal conductance for different thicknesses of graphene, but no systematic dependence on the thickness was found (Z. Chen *et al.*, 2009; Mak, Lui, and Heinz, 2010).

There exist far fewer measurements on the interfacial thermal conductance of other 2D materials. Jo *et al.* (2013) extracted both thermal conductivity of *h*-BN and the interfacial thermal conductance (~2 MW/m^2K) of *h*-BN on SiN_x substrate from their microbridge experiment. Liu, Choi, and Cahill (2014) showed that the interfacial thermal conductance between MoS_2 and aluminum, NbV and CoPt are 20, 25, and 26 MW/m^2K, respectively. These values are lower than the interfacial thermal conductance of Al film on highly ordered pyrolytic graphite. Taube *et al.* (2015) employed optothermal Raman measurements to extract the interfacial thermal conductance of single-layer MoS_2 on SiO_2. They found it to be ~1.9 MW/m^2K, which is comparable to that of *h*-BN on SiN_x.

There are also several efforts to control the interfacial thermal conductance between 2D materials and substrates. By corrugating a substrate, the interfacial thermal conductance between graphene and the substrate is reduced by 5 orders of magnitude relative to a seamless contact (Tang *et al.*, 2014). Even for a perfect interface contact, the interfacial thermal conductance can be actively tuned by applying an electrostatic field, which can improve the conformation between the graphene and substrate (Koh *et al.*, 2016).

III. THERMAL PROPERTIES OF NANOSTRUCTURES BASED ON 2D CRYSTALS

A. Defects and alloying

Imperfections, such as point defects, vacancies, and grain boundaries, inevitably occur in 2D materials. These imperfections usually lead to phonon-defect or phonon-boundary scattering and thus reduce the thermal conductivity.

Theoretically, the phonon scattering rate due to point defects can be derived from Fermi's golden rule (Tamura, 1983) or be calculated using Green's functions (Kundu *et al.*, 2011; Katcho *et al.*, 2014). For 2D crystals, the phonon scattering rate can be roughly estimated by (Klemens, 1955, 2000; Klemens and Pedraza, 1994)

$$1/\tau^{\mathrm{D}} \propto (\omega^{\alpha}/v^{\beta})\sum_{i} f_i[(1-M_i/\bar{M})^2+\epsilon(\gamma_{\mathrm{G}}(1-r_{a,i}/\bar{r}_a))^2], \tag{3}$$

where M_i, $r_{a,i}$, and f_i are the mass, radius, and fractional concentration of type i atom, $\bar{M}$ and $\bar{r}_a$ are the averaged atom mass and radius, γ_{G} is the Grüneisen parameter, v is the phonon group velocity, and ϵ is a phenomenological parameter characterizing the relative importance of defect scattering due to mass difference and lattice distortion. In Eq. (3), $\alpha = 3$ and $\beta = 2.5$ for a linear phonon dispersion and $\alpha = 2$ and $\beta = 1.5$ for a quadratic phonon dispersion, respectively. This expression indicates that the high-frequency (short-wavelength) phonon modes are more likely to be scattered by defects.

Chen *et al.* (2012) synthesized graphene sheets with different compositions of carbon isotopes ^{12}C and ^{13}C and measured their thermal conductivity. A small concentration (1.1%) of ^{13}C isotopes was found to lead to a 30% reduction in thermal conductivity. Pettes *et al.* (2015) experimentally studied the effects of isotope scattering on the measured thermal conductivity of high-quality ultrathin graphite samples at both low- and high-isotope impurity concentrations. The measured thermal conductivity of the samples was below the value predicted by an incoherent isotope-scattering model derived from perturbation theory, which was attributed to the effects of multiple scattering of phonons by high-concentration isotope impurities in low-dimensional systems. The effect of isotopes was also studied in other 2D materials, such as *h*-BN (Lindsay and Broido, 2011) and MoS_2 (Li, Carrete, and Mingo, 2013), through PBTE calculations. In addition to randomly distributed isotopes, Mingo *et al.* (2010) employed Green's functions to investigate the possibility of utilizing isotope clusters to tune the thermal conductivity of graphene. As scattering is sensitive to the size of the imperfections, the isotope clusters play a similar role to nanoparticles in bulk materials (Kim *et al.*, 2006), i.e., scattering low-frequency phonons and thus further reducing the thermal conductivity relative to naturally occurring graphene. The Green's function calculations show that isotope clustering results in a remarkable increase of the scattering cross section and thus a significant reduction of the thermal conductivity (Mingo *et al.*, 2010).

Equation (3) shows that introducing different kinds of atoms could more effectively scatter phonons than the isotopic counterparts, since it introduces both mass differences and lattice distortion. Indeed, lattice distortion in 2D materials could be quite different from that in 3D bulk materials when other kinds of atoms are introduced. An AGF calculation was carried out to investigate how phonons transmit across a Si defect in graphene (Jiang, Wang, and Wang, 2011a). With small phonon transmission across this defect, thermal conductivity is largely reduced.

Compared to isotopes and substitutions, vacancies can more effectively suppress the thermal conductivity (Hao, Fang, and Xu, 2011; Zhang, Lee, and Cho, 2011). For example, MD simulations by Hao, Fang, and Xu (2011) showed that the thermal conductivity of graphene with 1% vacancies is reduced to 10%–20% of unmodified graphenes, while only a reduction to 70% is found when 1% ^{12}C atoms are replaced by ^{13}C atoms (Chen *et al.*, 2012). Raman-based optothermal measurement of graphene with electron beam irradiation induced defects reveals a thermal conductivity reduction from 1800 to 400 W/mK near room temperature as the defect density is slightly changed from 2.0×10^{10} cm^{-2} (0.0005%) to 1.8×10^{11} cm^{-2} (0.005%) (Malekpour *et al.*, 2016).

From classical perturbation theory, if a vacancy is modeled as if one atom is removed from the crystal along with all the bonding associated with this atom, the effect of vacancy on phonon scattering rate can be estimated by (Ratsifaritana and Klemens, 1987)

$$\frac{1}{\tau^{\mathrm{V}}_{\mathbf{q}s}} \propto \frac{\delta^3}{G_{\mathrm{V}}}\frac{\omega^{\alpha}}{v^{\beta}}, \tag{4}$$

where G_{V} is the number of atoms per defect, δ^3 denotes the atomic volume, and α and β have the same meanings as in Eq. (3). Recently, Xie *et al.* (2014) pointed out that this classical model neglected the different characteristics of atomic bonds connecting the undercoordinated atoms, which have fewer neighbors to form bonds due to defects than the atoms in perfect crystal.

B. Heterostructures

Many efforts have been devoted to the synthesis of heterostructures based on a diverse set of 2D materials. Both in-plane and vertical heterostructures of TMDs have been synthesized (Duan *et al.*, 2014; Gong *et al.*, 2014). Thermal transport in such heterostructures has yet to be systematically studied, although there are a few studies on graphene/*h*-BN and graphene/silicene related structures using MD simulations (Kınacı *et al.*, 2012; Jing, Hu, and Guo, 2013; Song and Medhekar, 2013; Zhu and Ertekin, 2014; Gao, Liu, and Xu, 2016; Gao, Yang, and Xu, 2017) and the AGF approach (Jiang, Wang, and Wang, 2011b).

MD simulations showed that, for in-plane graphene/*h*-BN superlattices, the thermal conductivity along the direction of the graphene/*h*-BN interface is sensitive to the type of interface. If the graphene and *h*-BN stripes are connected by a zigzag edge, the thermal conductivity is larger than if they are connected by an armchair edge (Sevik *et al.*, 2011). The effect is more pronounced when the width of the stripe is small, but superlattices with both types of interfaces are found to converge to the average thermal conductivity of graphene and *h*-BN when the stripes are sufficiently wide. When the heat flux is perpendicular to the interface, the thermal conductivity of the in-plane superlattice of 2D crystals initially decreases with a decreasing superlattice period, then increases if the period is reduced further (Zhu and Ertekin, 2014). The minimum thermal conductivity was found to be at a critical period of 5 nm.

Thermal transport in graphene with embedded hexagonal *h*-BN quantum dots has been studied using both a real-space Kubo approach (Sevinçli *et al.*, 2011), where the phonon transmission is computed through the Kubo formula, and EMD simulations (Sevik *et al.*, 2011). Both studies showed that the thermal conductivity of graphene with quantum dots is reduced compared to pristine graphene. The reduction of the thermal conductivity is less distinct with larger quantum dots. The minimal thermal conductivity was found at 50% concentration of *h*-BN quantum dots with radii of 0.495, 1.238, and 2.476 nm.

Inspired by the high power factor of single-layer MoS_2, Gu and Yang (2016) introduced the concept of "nanodomains in 2D alloy" (which is an analog of the widely used "nanoparticles in alloy" approach for achieving a high thermoelectric figure of merit in 3D materials) to reduce the thermal conductivity of 2D crystals. The $Mo_{0.8}W_{0.2}S_2$ alloy embedded with 10-unit-cell-large triangular WS_2 nanodomains was shown to have only 10% of the intrinsic thermal conductivity of single-layer MoS_2, due to the strong alloy scattering for high-frequency phonons and the scattering of low-frequency phonons by WS_2 nanodomains. It was found that the minimum thermal conductivity alloy is not necessarily the best matrix material for such nanocomposites to achieve the lowest thermal conductivity, since there is a competition between alloy scattering and nanodomain scattering when the alloy is partially replaced with nanodomains. For some TMD alloys, for example, $Mo_{1-x}W_xTe_2$, the thermal conductivity could be further tuned by utilizing the composition-dependent phase transition (Yan *et al.*, 2017; Qian *et al.*, 2018).

The thermal conductance across interfaces between two different 2D materials in either vertical or in-plane heterostructures was also investigated. C.-C. Chen *et al.* (2014) measured the interfacial thermal conductance between vertically stacked graphene and *h*-BN using the optothermal Raman technique. They found that the interfacial thermal conductance is about 7.4 MW/m^2K at room temperature and attributed the measured low interfacial thermal conductance of *h*-BN/graphene to liquid or organic residues. They believed that the interfacial thermal conductance could be enhanced if the lattice mismatch during graphene growth on *h*-BN was minimized. MD simulations with a transient heating scheme were also performed to mimic the laser heating in the optothermal Raman measurement. An interfacial thermal conductance of *h*-BN/graphene was found to be 3.4 MW/m^2K, which is consistent with the optothermal Raman measurement (Zhang, Hong, and Yue, 2015). The simulations also showed that the interfacial thermal conductance could be increased by raising the temperature, increasing the bonding strength, or introducing graphene hydrogenation. A similar MD study showed that the thermal conductance of a graphene/MoS_2 interface is 5.8 MW/m^2K (Liu *et al.*, 2015). The interfacial thermal conductance of an in-plane interface between graphene and silicene was found to be 250 MW/m^2K using NEMD simulations (B. Liu *et al.*, 2014).

C. Surface functionalization and intercalation

Some 2D materials can be made by chemical functionalization of existing materials. Indeed, many graphene derivatives have been synthesized through hydrogenation, oxidization, or fluorination. Compared with single-layer pristine graphene, the calculated thermal conductivity of hydrogenated graphene (graphane) and fluorinated graphene (fluorographene) with a 100% coverage of the H and F atoms are reduced to 40%–50% (Pei, Sha, and Zhang, 2011; Kim, Lee, and Grossman, 2012; Liu *et al.*, 2012) and 35% (Huang *et al.*, 2012) in MD simulations and ∼50% and ∼7% in a first-principles-based PBTE study (Fugallo *et al.*, 2014), respectively. The phonon lifetimes of graphane, extracted from MD simulations, were found to be decreased by an order of magnitude compared with those in pristine graphene (Kim, Lee, and Grossman, 2012). The larger scattering rate is due to the coupling between the in-plane and out-of-plane phonon modes (Liu *et al.*, 2012). For some other carbon-based 2D materials, hydrogenation was found to enhance thermal conductivity. This enhancement is thought to be caused by hydrogenation induced anharmonicity reduction from the conversion of sp^2 bonding to sp^3 bonding.

Unlike in conventional thin film materials, thermal transport in functionalized graphene can also be tuned through the coverage of the functionalized molecules. When the coverage increases from 0% to 100%, the thermal conductivity generally exhibits a U-shaped curve (Pei, Sha, and Zhang, 2011; Huang *et al.*, 2012; Liu *et al.*, 2012), similar to the dependence of alloy thermal conductivity on its composition. Mu *et al.* (2014) showed that graphene oxide with 20% coverage has a thermal conductivity lower than the calculated thermal conductivity of graphene according to minimum thermal conductivity theory (Cahill, Watson, and Pohl, 1992).

Despite the fact that, in most carbon-based materials, the thermal conductivity is reduced after functionalization, Han *et al.* (2016) showed experimentally that a graphene film deposited on a functionalized graphane could serve as a high-performance heat spreader for electronic chips, which leads to a lower chip temperature than either a graphene film or a graphene film with nonfunctionalized graphane. Functionalization of graphane not only reduces the contact resistance between graphene and the substrate (chip), but also enhances the thermal conductivity of the graphene film by suppressing the substrate-graphene scattering for flexural phonon modes.

In addition to surface functionalization, intercalation is another facile chemical approach to tune the thermal properties of layered 2D materials. There has been a rich chemistry in intercalating 2D materials to form composites or superlattice of layered 2D materials (Wilson and Yoffe, 1969; Dresselhaus and Dresselhaus, 1981; Whittingham and Jacobson, 2012). Intercalation compounds are formed by the insertion of atomic or molecular layers of a different chemical species (called the intercalant) between the layers of a layered host material, such as graphite, transition metal dichalcogenides, or other van der Waals crystals. When the intercalants are inserted into the van der Waals gap of the layered material, charges can be transferred to the layers of the host materials (Wilson and Yoffe, 1969), leading to a change in the Fermi level and thus changing the electron density of states close to the Fermi level, which has tremendous impact on the applications in electronics, photonics, and electrochemical energy storage (Dresselhaus and Dresselhaus, 1981).

Besides changing the electronic properties, thermal conductivity also changes significantly from intercalation. Intercalation can change both the magnitude and anisotropy of the thermal conductivity. The study of thermal conductivity of intercalated compounds can be traced back to the 1980s (Elzinga, Morelli, and Uher, 1982; Issi, Heremans, and Dresselhaus, 1983; Clarke and Uher, 1984).

To explain the lower lattice thermal conductivity around room temperature, Issi, Heremans, and Dresselhaus (1983) employed the PBTE formalism, which considers the scattering of in-plane phonon modes in the intercalation compound's graphene layers (including phonon-phonon scattering, grain boundary scattering, and defect scattering). By fitting the experimental data to the analytical expressions of phonon relaxation times, they attributed the reduced thermal conductivity to the lattice distortion associated with large-scale defects and the grain boundary scattering. However, the extracted feature size of the grains is about 1 order of magnitude smaller than their experimental observation, indicating that there are additional scattering mechanisms not considered in their model. Recent MD simulations provided atomic-scale insight into the effect of lithium intercalation on the spectral phonon properties of graphite (Qian *et al.*, 2016). It was found that the intercalation of lithium ions tunes the anisotropy of graphite's thermal conductivity. The basal-plane thermal conductivity experiences a threefold reduction as lithium composition x increases from 0 to 1 in Li_xC_6 [Fig. 11(a)], while the c-axis thermal conductivity decreases from 6.5 (pristine graphite) to 1.8 W/mK (LiC_{18}), then increases back to 5.0 W/mK (LiC_6) when fully charged, as shown in Fig. 11(b). Figures 11(c) and 11(d) provide a comparison between pristine graphite and lithiated LiC_6. Li ion vibrations are plotted in gray, while the vibration of the graphite's carbon atoms are plotted in black. Clearly many low energy flat modes are introduced by lithium intercalation, and these modes gradually merge with the graphite host's vibrational modes. This significantly suppresses the in-plane phonon group velocities, reducing the basal-plane thermal conductivity. Such phonon hybridization is also observed in other materials (such as clathrates and skutterudites) with rattler atoms weakly coupled to their host material and found to be responsible for their low thermal conductivity. The nonmonotonic change of thermal conductivity along the c-axis direction is explained by two counteractive factors: First, the intercalated lithium ions induce extra electrostatic interaction via the charge transfer process. This enhanced interlayer coupling increases the phonon velocities along the c axis relative to pristine graphite, as shown in Figs. 11(e) and 11(f). Second, the lithium ions also provide extra phonon scattering channels, suppressing the phonon lifetime. These two opposing factors together render the nonmonotonic change in the thermal conductivity along the c axis.

Although many other intercalation compounds aside from graphite intercalation compounds have been synthesized, there are only limited thermal conductivity measurements. TiS_2-based intercalation compounds have attracted considerable attention due to the large thermoelectric power of bulk TiS_2 crystals (Imai, Shimakawa, and Kubo, 2001). Wan *et al.* (Wan, Wang, Wang, and Koumoto, 2010; Wan, Wang, Wang, Norimatsu *et al.*, 2010; Wan *et al.*, 2011, 2012) inserted different intercalants, such as SnS and BiS, into the TiS_2 van der Waals gap to form natural superlattices and demonstrated

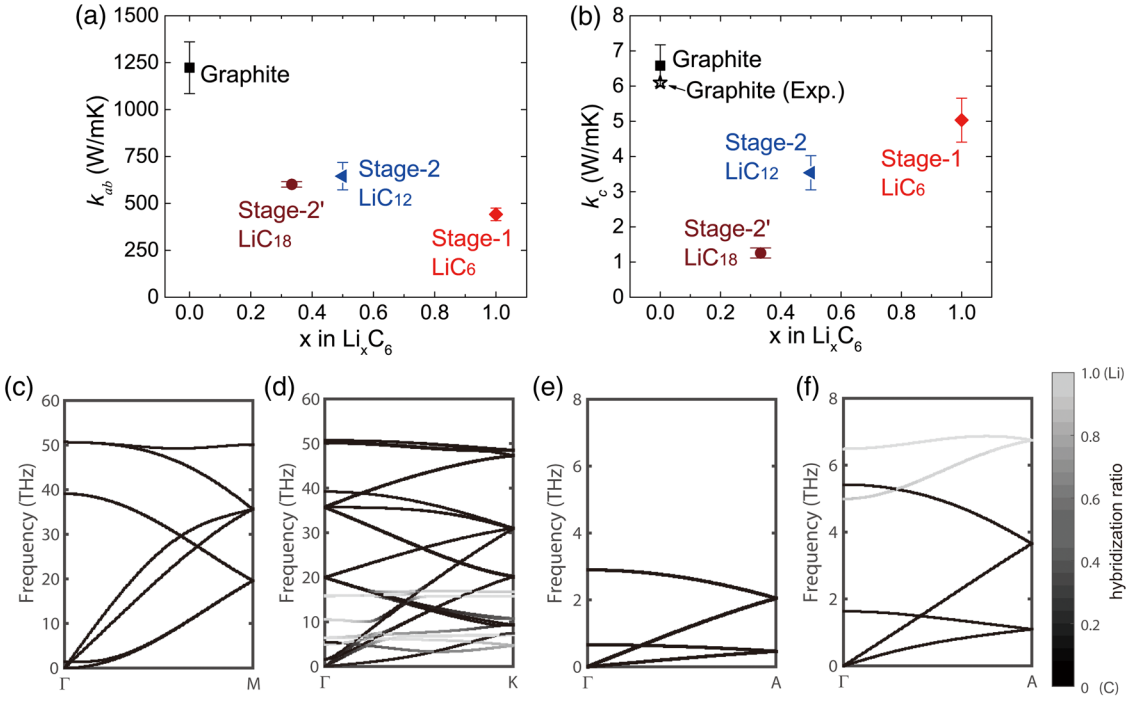

FIG. 11. (a) Basal-plane thermal conductivity and (b) thermal conductivity along the c axis as a function of lithium composition. The experimental data are taken from Schmidt, Chen, and Chen (2008). (c), (d) Comparison of phonon dispersion in the basal plane of pristine graphite and LiC_6. (e), (f) Comparison of phonon dispersion along the c axis of pristine graphite and LiC_6. Adapted from Qian *et al.*, 2016.

an improved thermoelectric figure of merit. One example is the superlattice $(SnS)_1(TiS_2)_2$, where the SnS layer is intercalated into the TiS_2 layered crystal. The cross-plane thermal conductivity is shown to be lower than the prediction of the minimum thermal conductivity theory. They attributed this low thermal conductivity to phonon localization due to the orientation disorder of the SnS layers (Wan *et al.*, 2011).

Organic molecules can also be inserted into the van der Waals gaps. Wan *et al.* recently synthesized $TiS_2/[(\text{hexylammonium})_{0.08}(H_2O)_{0.22}(DMSO)_{0.03}]$ (an inorganic/organic layered hybrid material) for thermoelectric applications (Wan, Gu *et al.*, 2015; Wan, Kodama *et al.*, 2015) [Fig. 12(a)]. Because of its low lattice thermal conductivity [Fig. 12(b)] and relatively unchanged power factor from TiS_2 crystals, the thermoelectric figure of merit is measured to be as high as 0.42, making the hybrid organic-inorganic superlattice a promising *n*-type flexible thermoelectric material (Wan, Gu *et al.*, 2015). The measured thermal conductivity of the hybrid material is only one-sixth of that of the bulk counterpart. More surprisingly, the lattice thermal conductivity was only 1/30 of bulk TiS_2 after using the Weidmann-Franz law to extract the electronic contribution. MD simulations were performed to calculate the thermal conductivity of bulk TiS_2 and hybrid organic-inorganic materials and an eightfold reduction of lattice thermal conductivity was found for TiS_2 when intercalated with organic components. This reduction is significantly higher than simple volumetric averaging, indicating that the inorganic-organic coupling plays an important role in the in-plane phonon transport.

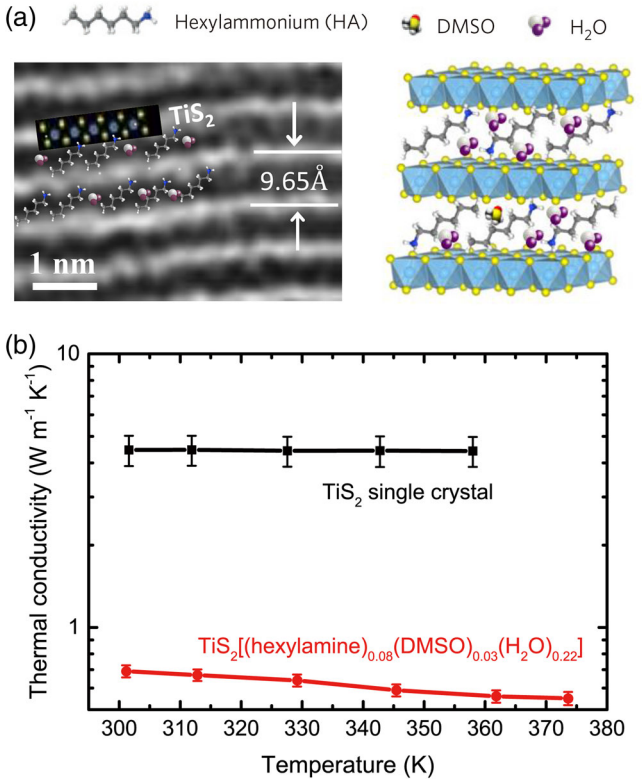

FIG. 12. (a) High angle annular dark field scanning transmission electron microscopy image of $TiS_2[(HA)_x(H_2O)_y(DMSO)_z]$ along with the schematic atomic structure. (b) Measured in-plane thermal conductivity. Adapted from Wan, Gu *et al.*, 2015.

The thermal conductivity of lithium-intercalated compounds of cobalt oxide (Cho *et al.*, 2014) and MoS_2 (G. Zhu *et al.*, 2016) were recently measured using the transient thermoreflectance technique. The thermal conductivity of both compounds was found to be tunable with the amount of Li ions intercalated. In particular, intercalation of lithium changes the thermal conductivity anisotropy in MoS_2 (G. Zhu *et al.*, 2016). The basal-plane thermal conductivity decreases monotonically but the cross-plane thermal conductivity decreases and then increases with increasing lithium composition. This experimental trend was found to be similar to MD simulation results for the lithium-intercalated graphite compounds (Qian *et al.*, 2016).

IV. SUMMARY AND OUTLOOK

A. Summary

Through a comprehensive survey of a large body of literature, we have answered most of the questions on phonon and thermal properties in 2D materials raised at the beginning of this Colloquium.

(a) In general, the phononic thermal conductivity of a suspended 2D material keeps increasing with the sample size even when the size is beyond tens of microns. Some first-principles calculations suggested that it converges when the sample is about 1 mm. However, this has not yet been experimentally confirmed. Strain and crystal structure can significantly affect the scattering of long-wavelength acoustic phonons, complicating the thermal conductivity's length dependence.

(b) For suspended 2D materials, thermal conductivity decreases with the increasing number of layers because interlayer interactions suppress the flexural modes. For some 2D crystals, the thickness dependence of thermal conductivity can exhibit a different trend due to the distinct crystal structures and the corresponding phonon dispersion and scattering properties.

(c) The thermal conductivity of any supported 2D materials is a finite value because of the suppression of flexural modes and the breakdown of the translational invariance. The thermal conductivity of 2D materials and the interfacial thermal conductance can be modulated by a substrate. When the structure of the substrate is very similar to that of 2D materials, the reduction is minimized. Mechanical strain plays an important role in modulating thermal conductivity.

(d) Defects and functionalization can considerably reduce thermal conductivity of 2D materials. Intercalation could affect both the group velocities and phonon relaxation times of layered crystals, thus tuning the thermal conductivity along the through-plane and basal-plane directions.

Many remarkable achievements and progress has been made in the past decade on phonon and thermal properties of 2D materials including graphene, however, there are still many challenging theoretical and experimental questions that need to be solved.

Theoretically, there is no rigorous mathematical proof on whether there exists size dependence of intrinsic thermal conductivity of 2D materials. The modeling of 2D lattices has been limited to the in-plane motion of lattices (Lippi and Livi, 2000; Yang, Grassberger, and Hu, 2006; Xiong *et al.*, 2010; Wang, Hu, and Li, 2012). This simplification is used because theoretical analysis (e.g., mode-mode coupling) becomes extremely difficult when flexural modes are considered. However, in order to understand thermal transport in realistic 2D materials, the flexural motion should not be neglected. In the meantime, significant progress has been made in the study of heat conduction in a 1D system over the last few decades. With great effort from both mathematicians and theoretical physicists, we now know that thermal conductivity in 1D momentum conserved systems can exhibit anomalous behavior, although more experimental works are still needed to verify this theoretical predication. We hope that this summary of the anomalous heat conduction behavior in 2D systems and 2D materials (even if it is only up to a certain length) in this Colloquium can help attract attention from theoreticians and experimentalists.

Experimentally, only limited techniques are available for measuring thermal conductivity of 2D materials. The optothermal Raman spectroscopy that was used to obtain the first experimental data on thermal conductivity of suspended single-layer graphene has been found to overestimate thermal conductivity. This method relies on two conditions: (1) absorption of laser energy by the materials and (2) the temperature dependence of the phonon peak shift. Any wrong calculation of these two factors could result in a significant systematic error. The first one has been known for many years, however, the second one has only been investigated recently by Vallabhaneni *et al.* (2016). In their detailed computational study, Vallabhaneni *et al.* pointed out that the ZA and ZO phonons that contribute the most to the thermal conductivity of single-layer graphene are indeed out of thermal equilibrium. The temperature of these phonon modes is found to be much lower than the temperature measured from the shift of Raman peak frequency. The latter is assumed to be the equilibrium lattice temperature. This leads to an overestimate of the thermal conductivity by a factor of 1.35–2.6 at room temperature. How to incorporate such theoretical understanding into optothermal Raman spectroscopy to obtain a more accurate measurement of thermal conductivity is an interesting new direction (Sullivan *et al.*, 2017).

B. Outlook

1. Dimensional crossover from 2D to 1D and from 2D to 3D

2D materials provide an ideal test platform to study the dimensional crossover of phonon transport. When studying the size effect of 2D materials, in principle we simultaneously change both the width and length of samples to preserve the two dimensionality. However, in experiments it is often more convenient to keep the width fixed and only the length is changed. Indeed this could be an effective way to study the dimensional crossover from 2D to 1D. A transition signature was reported in a recent experiment on thermal conductivity versus length for a suspended single-layer graphene (Xu *et al.*, 2014). It could also be interesting to know how many layers are necessary to render a bulk thermal conductivity of layered materials.

2. Electronic thermal transport

Electrons also carry heat in both metals and semiconductors. In bulk materials, the electronic thermal conductivity and electrical conductivity are related by the well-known Wiedemann-Franz law (Kittel, 2005). However, in low-dimensional systems, as discussed in this Colloquium, heat conduction becomes anomalous and it is not clear if the Wiedemann-Franz law is still valid. Lee *et al.* (2017) recently found that at 240–340 K the Wiedmann-Franz law is broken in metallic vanadium dioxide (VO_2). There is no doubt that there might also be anomalous thermal transport for electrons in 2D materials.

3. Electron-phonon coupling

It is known that in both the Raman optothermal method and the other laser heating and probing methods, the heating energy is transferred first from photons to electrons, and then from electrons to phonons through electron-phonon coupling. The electron-phonon coupling determines how much energy can be transferred from hot electrons to phonons. The coupling also determines the temperature of the phonons, if nonequilibrium transport is neglected by assuming a sufficiently long time window in thermal metrology. A better understanding of electron-phonon coupling in 2D materials helps to improve the measurement accuracy of thermal conductivity.

4. Topological phonon effect in 2D materials

2D materials provide a test platform for the topological phonon effect. The phonon Hall effect was discovered (Strohm, Rikken, and Wyder, 2005; Inyushkin and Taldenkov, 2007) in crystals of paramagnetic terbium gallium garnet, $Tb_3Ga_5O_{12}$. These cubic crystals are dielectrics and contain ions that carry both a high charge and a large magnetic moment; both factors may induce a strong coupling to an applied magnetic field, leading to the phonon Hall effect.

A theoretical study by Zhang *et al.* (2010) showed that on a 2D honeycomb lattice the phonon Hall effect arises due to the Berry phase induced by the band curvature. Moreover, this phase is quantized in the multiples of the Chern number indicating that the phonon Hall effect is intrinsically a topological effect. Additional analysis by Qin, Zhou, and Shi (2012) confirmed that the thermal conductivity in the Hall regime is the same as that of a series of 1D quantum wires, which is consistent with the expectation that a topological material develops nontrivial edge modes.

The phonon Hall effect remains unexplored in many realistic 2D materials, both theoretically and experimentally. In particular, in magnetically ordered materials such as yttrium iron garnet, the presence of strong magnetoelastic spin-phonon couplings allows the hybridization of magnons and phonons.

5. Phononic quantum devices with 2D materials

The novel characteristics of phonons in 2D materials can find applications in an emerging field of quantum engineering. Because of their extremely low mass, 2D materials have been used as a nanoscale membrane to build a nanoscale drum (optomechanical cavity), which enables quantum information storage. Moreover, 2D materials can be used as optomechanical sensors with unprecedented sensitivities. For example, Singh *et al.* (2014) demonstrated a displacement sensitivity of 17 $\mathrm{fm/Hz^{1/2}}$ when a multilayer graphene resonator, with $Q = 220\,000$, is coupled to a high Q superconducting cavity. The results show a potential for phonon storage for up to 10 ms, a significant improvement compared with other mechanical resonators such as silicon microsphere (3 μs) (Fiore *et al.*, 2011), and superconducting aluminum membrane (90 μs) (Palomaki *et al.*, 2013). In addition to the quantum storage demonstrated by Singh *et al.* (2014), propagating phonons can also be used to transmit quantum information when coupled to artificial atoms in the quantum regime (Gustafsson *et al.*, 2014). These works have opened a new direction of phonons in quantum information and computation (Aspelmeyer, Kippenberg, and Marquardt, 2014; Tian, 2015).

6. Anomalous thermal conductivity and the second sound

Another interesting topic worth exploring is whether the anomalous thermal conductivity in 2D materials has any connection with the second sound—a transport of heat in the form of a wave. The second sound is a spatially periodic fluctuation of entropy and temperature. This is different from conventional sound, an acoustic wave that is a periodic fluctuation of mass density and pressure. The second sound concept was proposed (Donnelly, 2009) for helium II where both the normal fluid and superfluid coexist, and has been experimentally observed in hydrodynamic materials such as solid helium (Ackerman *et al.*, 1966), NaF (Jackson, Walker, and McNelly, 1970; Pohl and Irniger, 1976), bismuth (Narayanamurti and Dynes, 1972), and $SrTiO_3$ (Koreeda, Takano, and Saikan, 2007) at very low temperature. A theoretical question one would naturally ask is whether the second sound exists in 2D materials at room temperature. There have been some theoretical studies along this direction (Cepellotti *et al.*, 2015; Lee, Broido *et al.*, 2015). It would be interesting to study this experimentally if the speed of the second sound can be probed.

ACKNOWLEDGMENTS

B. L. thanks J. Chen, D. Donadio, B. Hu, S.-Q. Hu, W. Li, D. Liu, B. Özyilmaz, J. Ren, J. T. L. Thong, J.-S. Wang, J.-Y. Wang, L. Wang, R.-G. Xie, X.-F. Xu, N. Yang, G. Zhang, L.-F. Zhang, Z.-W. Zhang, and L.-Y. Zhu for fruitful collaborations in 2D systems. R. Y. thanks M. S. Dresselhaus, P. Q. Jiang, Y. K. Koh, K. Koumoto, X. B. Li, J. Liu, X. Qian, C. L. Wan, X. J. Wang, and J. Zhu for their collaborative work on thermal transport in 2D materials over the past 10 years or so. We thank S. R. Sklan for reviewing and editing the final version of this article. The funding support for R. Y. was provided by the National Science Foundation (Grants No. 0846561 and No. 1512776) and DARPA (Grant No. FA8650-15-1-7524). Y. W. acknowledges the support from the National Natural Science Foundation of China (Grant No. 11425211) and the Strategic Priority Research Program of the Chinese Academy of Sciences (No. XDB22020200).

REFERENCES

Ackerman, C. C., B. Bertman, H. A. Fairbank, and R. Guyer, 1966, "Second sound in solid helium," Phys. Rev. Lett. **16**, 789.

Aksamija, Z., and I. Knezevic, 2011, "Lattice thermal conductivity of graphene nanoribbons: Anisotropy and edge roughness scattering," Appl. Phys. Lett. **98**, 141919.

Alam, M., R. Pulavarthy, C. Muratore, and M. A. Haque, 2015, "Mechanical strain dependence of thermal transport in amorphous silicon thin films," Nanoscale Micro. Thermophys. Eng. **19**, 1.

Ashcroft, N. W., and N. D. Mermin, 1978, *Solids State Physics* (Holt, Rinehart and Winston, New York).

Aspelmeyer, M., T. J. Kippenberg, and F. Marquardt, 2014, "Cavity optomechanics," Rev. Mod. Phys. **86**, 1391.

Bae, M. H., Z. Li, Z. Aksamija, P. N. Martin, F. Xiong, Z. Y. Ong, I. Knezevic, and E. Pop, 2013, "Ballistic to diffusive crossover of heat flow in graphene ribbons," Nat. Commun. **4**, 1734.

Balandin, A. A., 2011, "Thermal properties of graphene and nanostructured carbon materials," Nat. Mater. **10**, 569.

Balandin, A. A., S. Ghosh, W. Bao, I. Calizo, D. Teweldebrhan, F. Miao, and C. N. Lau, 2008, "Superior thermal conductivity of single-layer graphene," Nano Lett. **8**, 902.

Barbarino, G., C. Melis, and L. Colombo, 2015, "Intrinsic thermal conductivity in monolayer graphene is ultimately upper limited: A direct estimation by atomistic simulations," Phys. Rev. B **91**, 035416.

Berciaud, S., S. Ryu, L. E. Brus, and T. F. Heinz, 2009, "Probing the intrinsic properties of exfoliated graphene: Raman spectroscopy of free-standing monolayers," Nano Lett. **9**, 346.

Bhowmick, S., and V. B. Shenoy, 2006, "Effect of strain on the thermal conductivity of solids," J. Chem. Phys. **125**, 164513.

Bonini, N., J. Garg, and N. Marzari, 2012, "Acoustic phonon lifetimes and thermal transport in free-standing and strained graphene," Nano Lett. **12**, 2673.

Broido, D., M. Malorny, G. Birner, N. Mingo, and D. Stewart, 2007, "Intrinsic lattice thermal conductivity of semiconductors from first principles," Appl. Phys. Lett. **91**, 231922.

Broido, D., A. Ward, and N. Mingo, 2005, "Lattice thermal conductivity of silicon from empirical interatomic potentials," Phys. Rev. B **72**, 014308.

Cahill, D. G., S. K. Watson, and R. O. Pohl, 1992, "Lower limit to the thermal conductivity of disordered crystals," Phys. Rev. B **46**, 6131.

Cai, W., A. L. Moore, Y. Zhu, X. Li, S. Chen, L. Shi, and R. S. Ruoff, 2010, "Thermal transport in suspended and supported monolayer graphene grown by chemical vapor deposition," Nano Lett. **10**, 1645.

Cao, H.-Y., Z.-X. Guo, H. Xiang, and X.-G. Gong, 2012, "Layer and size dependence of thermal conductivity in multilayer graphene nanoribbons," Phys. Lett. A **376**, 525.

Carrete, J., W. Li, L. Lindsay, D. A. Broido, L. J. Gallego, and N. Mingo, 2016, "Physically founded phonon dispersions of few-layer materials and the case of borophene," Mater. Res. Lett. **4**, 204.

Castellanos-Gomez, A., L. Vicarelli, E. Prada, J. O. Island, K. Narasimha-Acharya, S. I. Blanter, D. J. Groenendijk, M. Buscema,

G. A. Steele, and J. Alvarez, 2014, "Isolation and characterization of few-layer black phosphorus," 2D Mater. **1**, 025001.
Cepellotti, A., G. Fugallo, L. Paulatto, M. Lazzeri, F. Mauri, and N. Marzari, 2015, "Phonon hydrodynamics in two-dimensional materials," Nat. Commun. **6**, 6400.
Chang, C.-W., 2016, in *Experimental Probing of Non-Fourier Thermal Conductors*, edited by S. Lepri (Springer International Publishing, New York), p. 305.
Chen, C.-C., Z. Li, L. Shi, and S. B. Cronin, 2014, "Thermal interface conductance across a graphene/hexagonal boron nitride heterojunction," Appl. Phys. Lett. **104**, 081908.
Chen, G., 2001, "Ballistic-diffusive heat-conduction equations," Phys. Rev. Lett. **86**, 2297.
Chen, G., 2005, *Nanoscale Energy Transport and Conversion: A Parallel Treatment of Electrons, Molecules, Phonons, and Photons* (Oxford University Press, New York).
Chen, J., S. Chen, and Y. Gao, 2016, "Anisotropy Enhancement of Thermal Energy Transport in Supported Black Phosphorene," J. Phys. Chem. Lett. **7**, 2518.
Chen, J., G. Zhang, and B. Li, 2013, "Substrate coupling suppresses size dependence of thermal conductivity in supported graphene," Nanoscale **5**, 532.
Chen, L., and S. Kumar, 2012, "Thermal transport in graphene supported on copper," J. Appl. Phys. **112**, 043502.
Chen, S., *et al.*, 2011, "Raman measurements of thermal transport in suspended monolayer graphene of variable sizes in vacuum and gaseous environments," ACS Nano **5**, 321.
Chen, S., Q. Wu, C. Mishra, J. Kang, H. Zhang, K. Cho, W. Cai, A. A. Balandin, and R. S. Ruoff, 2012, "Thermal conductivity of isotopically modified graphene," Nat. Mater. **11**, 203.
Chen, S., Y. Zhang, J. Wang, and H. Zhao, **2016**, "Key role of asymmetric interactions in low-dimensional heat transport," J. Stat. Mech. 03, 033205.
Chen, Y., *et al.*, 2009, "Experimental realization of a three-dimensional topological insulator, Bi_2Te_3," Science **325**, 178.
Chen, Z., W. Jang, W. Bao, C. N. Lau, and C. Dames, 2009, "Thermal contact resistance between graphene and silicon dioxide," Appl. Phys. Lett., **95**, 161910.
Cho, J., M. D. Losego, H. G. Zhang, H. Kim, J. Zuo, I. Petrov, D. G. Cahill, and P. V. Braun, 2014, "Electrochemically tunable thermal conductivity of lithium cobalt oxide," Nat. Commun. **5**, 4035.
Clarke, R., and C. Uher, 1984, "High pressure properties of graphite and its intercalation compounds," Adv. Phys. **33**, 469.
Cocemasov, A. I., D. L. Nika, and A. A. Balandin, 2015, "Engineering of the thermodynamic properties of bilayer graphene by atomic plane rotations: the role of the out-of-plane phonons," Nanoscale **7**, 12851.
Conley, H. J., B. Wang, J. I. Ziegler, R. F. Haglund, Jr., S. T. Pantelides, and K. I. Bolotin, 2013, "Bandgap Engineering of Strained Monolayer and Bilayer MoS_2," Nano Lett. **13**, 3626.
Das, S. G., A. Dhar, and O. Narayan, 2014, "Heat Conduction in the $\alpha-\beta$ Fermi–Pasta–Ulam Chain," J. Stat. Phys. **154**, 204.
Dhar, A., 2008, "Heat transport in low-dimensional systems," Adv. Phys. **57**, 457.
Ding, Z., Q.-X. Pei, J.-W. Jiang, and Y.-W. Zhang, 2015, "Manipulating the thermal conductivity of monolayer MoS_2 via lattice defect and strain engineering," J. Phys. Chem. C **119**, 16358.
Donnelly, R. J., 2009, "The two-fluid theory and second sound in liquid helium," Phys. Today **62**, 34.
Dresselhaus, M. S., and G. Dresselhaus, 1981, "Intercalation compounds of graphite," Adv. Phys. **30**, 139.
Duan, X., *et al.*, 2014, "Lateral epitaxial growth of two-dimensional layered semiconductor heterojunctions," Nat. Nanotechnol. **9**, 1024.
Ecsedy, D. J., and P. G. Klemens, 1977, "Thermal resistivity of dielectric crystals due to four-phonon processes and optical modes," Phys. Rev. B **15**, 5957.
Elzinga, M., D. Morelli, and C. Uher, 1982, "Thermal transport properties of $SbCl_5$ graphite," Phys. Rev. B **26**, 3312.
Ernst, M., E. Hauge, and J. Van Leeuwen, 1971, "Asymptotic time behavior of correlation functions. I. Kinetic terms," Phys. Rev. A **4**, 2055.
Ernst, M., E. Hauge, and J. Van Leeuwen, 1976a, "Asymptotic time behavior of correlation functions. II. Kinetic and potential terms," J. Stat. Phys. **15**, 7.
Ernst, M., E. Hauge, and J. Van Leeuwen, 1976b, "Asymptotic time behavior of correlation functions. III. Local equilibrium and mode-coupling theory," J. Stat. Phys. **15**, 23.
Esfarjani, K., G. Chen, and H. T. Stokes, 2011, "Heat transport in silicon from first-principles calculations," Phys. Rev. B **84**, 085204.
Evans, W. J., L. Hu, and P. Keblinski, 2010, "Thermal conductivity of graphene ribbons from equilibrium molecular dynamics: Effect of ribbon width, edge roughness, and hydrogen termination," Appl. Phys. Lett. **96**, 203112.
Fan, Z., L. F. C. Pereira, P. Hirvonen, M. M. Ervasti, K. R. Elder, D. Donadio, T. Ala-Nissila, and A. Harju, 2017, "Thermal conductivity decomposition in two-dimensional materials: Application to graphene," Phys. Rev. B **95**, 144309.
Fasolino, A., J. H. Los, and M. I. Katsnelson, 2007, "Intrinsic ripples in grapheme," Nat. Mater. **6**, 858.
Faugeras, C., B. Faugeras, M. Orlita, M. Potemski, R. R. Nair, and A. Geim, 2010, "Thermal conductivity of graphene in corbino membrane geometry," ACS Nano **4**, 1889.
Feng, T., L. Lindsay, and X. L. Ruan 2017, "Four-phonon scattering significantly reduces intrinsic thermal conductivity of solids," Phys. Rev. B **96**, 161201(R).
Ferrari, A., *et al.*, 2006, "Raman spectrum of graphene and graphene layers," Phys. Rev. Lett. **97**, 187401.
Fiore, V., Y. Yang, M. C. Kuzyk, R. Barbour, L. Tian, and H. Wang, 2011, "Storing optical information as a mechanical excitation in a silica optomechanical resonator," Phys. Rev. Lett. **107**, 133601.
Fleurial, J. P., L. Gailliard, R. Triboulet, H. Scherrer, and S. Scherrer, 1988, "Thermal properties of high quality single crystals of bismuth telluride—Part I: Experimental characterization," J. Phys. Chem. Solids **49**, 1237.
Fu, Q., J. Yang, Y. Chen, D. Li, and D. Xu, 2015, "Experimental evidence of very long intrinsic phonon mean free path along the c-axis of graphite," Appl. Phys. Lett. **106**, 031905.
Fugallo, G., A. Cepellotti, L. Paulatto, M. Lazzeri, N. Marzari, and F. Mauri, 2014, "Thermal conductivity of graphene and graphite: collective excitations and mean free paths," Nano Lett. **14**, 6109.
Fugallo, G., M. Lazzeri, L. Paulatto, and F. Mauri, 2013, "Ab initio variational approach for evaluating lattice thermal conductivity," Phys. Rev. B **88**, 045430.
Gao, Y., Q.-C. Liu, and B.-X. Xu, 2016, "Lattice Mismatch Dominant Yet Mechanically Tunable Thermal Conductivity in Bilayer Heterostructures," ACS Nano, **10**, 5431.
Gao, Y., W. Z. Yang, and B.-X. Xu, 2017, "Tailoring Auxetic and Contractile Graphene to Achieve Interface Structures with Fully Mechanically Controllable Thermal Transports," Adv.Mater. Interfaces **4**, 1700278.
Garg, J., N. Bonini, B. Kozinsky, and N. Marzari, 2011, "Role of disorder and anharmonicity in the thermal conductivity of silicon-germanium alloys: A first-principles study," Phys. Rev. Lett. **106**, 045901.

Gendelman, O. V., and A. V. Savin, 2000, "Normal Heat Conductivity of the One-Dimensional Lattice with Periodic Potential of Nearest-Neighbor Interaction," Phys. Rev. Lett. **84**, 2381.

Gendelman, O. V., and A. V. Savin, 2014, "Normal heat conductivity in chains capable of dissociation," Europhys. Lett. **106**, 34004.

Ghosh, S., W. Bao, D. L. Nika, S. Subrina, E. P. Pokatilov, C. N. Lau, and A. A. Balandin, 2010, "Dimensional crossover of thermal transport in few-layer graphene," Nat. Mater. **9**, 555.

Giardina, C., R. Livi, A. Politi, and M. Vassalli, 2000, "Finite Thermal Conductivity in 1D Lattices," Phys. Rev. Lett. **84**, 2144.

Gong, Y., J. Lin, X. Wang, G. Shi, S. Lei, Z. Lin, X. Zou, G. Ye, R. Vajtai, and B. I. Yakobson, 2014, "Vertical and in-plane heterostructures from WS_2/MoS_2 monolayers," Nat. Mater. **13**, 1135.

Goyal, V., D. Teweldebrhan, and A. A. Balandin, 2010, "Mechanically-Exfoliated Stacks of Thin Films of Bismuth Telluride Topological Insulators with Enhanced Thermoelectric Performance," Appl. Phys. Lett., **97**, 133117.

Gu, X., B. Li, and R. G. Yang, 2016, "Layer thickness-dependent phonon properties and thermal conductivity of MoS_2," J. Appl. Phys. **119**, 085106.

Gu, X., and R. G. Yang, 2014, "Phonon transport in single-layer transition metal dichalcogenides: A first-principles study," Appl. Phys. Lett. **105**, 131903.

Gu, X., and R. G. Yang, 2015, "First-principles prediction of phononic thermal conductivity of silicene: A comparison with graphene," J. Appl. Phys. **117**, 025102.

Gu, X., and R. G. Yang, 2016, "Phonon transport in single-layer $Mo_{1-x}W_xS_2$ alloy embedded with WS_2 nanodomains," Phys. Rev. B **94**, 075308.

Guo, Z., D. Zhang, and X.-G. Gong, 2009, "Thermal conductivity of graphene nanoribbons," Appl. Phys. Lett. **95**, 163103.

Gustafsson, M. V., T. Aref, A. F. Kockum, M. K. Ekström, G. Johansson, and P. Delsing, 2014, "Propagating phonons coupled to an artificial atom," Science **346**, 207.

Han, H., *et al.*, 2016, "Functionalization mediates heat transport in graphene nanoflakes," Nat. Commun. **7**, 11281.

Hao, F., D. Fang, and Z. Xu, 2011, "Mechanical and thermal transport properties of graphene with defects," Appl. Phys. Lett. **99**, 041901.

Haskins, J., A. Kınacı, C. Sevik, H. l. Sevinçli, G. Cuniberti, and T. Çağın, 2011, "Control of thermal and electronic transport in defect-engineered graphene nanoribbons," ACS Nano **5**, 3779.

Henry, A., and G. Chen, 2008, "High thermal conductivity of single polyethylene chains using molecular dynamics simulations," Phys. Rev. Lett. **101**, 235502.

Henry, A., and G. Chen, 2009, "Anomalous heat conduction in polyethylene chains: Theory and molecular dynamics simulations," Phys. Rev. B **79**, 144305.

Hossain, M. S., F. Al-Dirini, F. M. Hossain, and E. Skafidas, 2015, "High performance graphene nano-ribbon thermoelectric devices by incorporation and dimensional tuning of nanopores," Sci. Rep. **5**, 11297.

Hsieh, W.-P., B. Chen, J. Li, P. Keblinski, and D. G. Cahill, 2009, "Pressure tuning of the thermal conductivity of the layered muscovite crystal," Phys. Rev. B **80**, 180302.

Hsieh, W.-P., M. D. Losego, P. V. Braun, S. Shenogin, P. Keblinski, and D. G. Cahill, 2011, "Testing the minimum thermal conductivity model for amorphous polymers using high pressure," Phys. Rev. B **83**, 174205.

Hu, J., X. Ruan, and Y. P. Chen, 2009, "Thermal conductivity and thermal rectification in graphene nanoribbons: a molecular dynamics study," Nano Lett. **9**, 2730.

Hu, J., S. Schiffli, A. Vallabhaneni, X. Ruan, and Y. P. Chen, 2010, "Tuning the thermal conductivity of graphene nanoribbons by edge passivation and isotope engineering: A molecular dynamics study," Appl. Phys. Lett. **97**, 133107.

Huang, W., Q.-X. Pei, Z. Liu, and Y.-W. Zhang, 2012, "Thermal conductivity of fluorinated graphene: A non-equilibrium molecular dynamics study," Chem. Phys. Lett. **552**, 97.

Imai, H., Y. Shimakawa, and Y. Kubo, 2001, "Large thermoelectric power factor in TiS 2 crystal with nearly stoichiometric composition," Phys. Rev. B **64**, 241104.

Inyushkin, A. V. e., and A. Taldenkov, 2007, "On the phonon Hall effect in a paramagnetic dielectric," JETP Lett. **86**, 379.

Issi, J.-P., J. Heremans, and M. S. Dresselhaus, 1983, "Electronic and lattice contributions to the thermal conductivity of graphite intercalation compounds," Phys. Rev. B **27**, 1333.

Jackson, H. E., C. T. Walker, and T. F. McNelly, 1970, "Second sound in NaF," Phys. Rev. Lett. **25**, 26.

Jain, A., and A. J. McGaughey, 2015, "Strongly anisotropic in-plane thermal transport in single-layer black phosphorene," Sci. Rep. **5**, 8501.

Jang, H., J. D. Wood, C. R. Ryder, M. C. Hersam, and D. G. Cahill, 2015, "Anisotropic thermal conductivity of exfoliated black phosphorus," Adv. Mater. **27**, 8017.

Jang, W., W. Bao, L. Jing, C. Lau, and C. Dames, 2013, "Thermal conductivity of suspended few-layer graphene by a modified T-bridge method," Appl. Phys. Lett. **103**, 133102.

Jiang, J.-W., H. S. Park, and T. Rabczuk, 2013, "Molecular dynamics simulations of single-layer molybdenum disulphide (MoS_2): Stillinger-Weber parametrization, mechanical properties, and thermal conductivity," J. Appl. Phys. **114**, 064307.

Jiang, J.-W., B.-S. Wang, and J.-S. Wang, 2011a, "First principle study of the thermal conductance in graphene nanoribbon with vacancy and substitutional silicon defects," Appl. Phys. Lett. **98**, 113114.

Jiang, J.-W., J.-S. Wang, and B.-S. Wang, 2011b, "Minimum thermal conductance in graphene and boron nitride superlattice," Appl. Phys. Lett. **99**, 043109.

Jing, L., M. Hu, and L. Guo, 2013, "Thermal conductivity of hybrid graphene/silicon heterostructures," J. Appl. Phys. **114**, 153518.

Jo, I., M. T. Pettes, J. Kim, K. Watanabe, T. Taniguchi, Z. Yao, and L. Shi, 2013, "Thermal conductivity and phonon transport in suspended few-layer hexagonal boron nitride," Nano Lett. **13**, 550.

Jo, I., M. T. Pettes, E. Ou, W. Wu, and L. Shi, 2014, "Basal-plane thermal conductivity of few-layer molybdenum disulfide," Appl. Phys. Lett. **104**, 201902.

Ju, Y., and K. Goodson, 1999, "Phonon scattering in silicon films with thickness of order 100 nm," Appl. Phys. Lett. **74**, 3005.

Katcho, N., J. Carrete, W. Li, and N. Mingo, 2014, "Effect of nitrogen and vacancy defects on the thermal conductivity of diamond: An ab initio Green's function approach," Phys. Rev. B **90**, 094117.

Kim, J. Y., J.-H. Lee, and J. C. Grossman, 2012, "Thermal transport in functionalized graphene," ACS Nano **6**, 9050.

Kim, P., L. Shi, A. Majumdar, and P. L. McEuen 2001, "Thermal Transport Measurements of Individual Multiwalled Nanotubes," Phys. Rev. Lett. **87**, 215502.

Kim, W., J. Zide, A. Gossard, D. Klenov, S. Stemmer, A. Shakouri, and A. Majumdar, 2006, "Thermal conductivity reduction and thermoelectric figure of merit increase by embedding nanoparticles in crystalline semiconductors," Phys. Rev. Lett. **96**, 045901.

Kınacı, A., J. B. Haskins, C. Sevik, and T. Çağın, 2012, "Thermal conductivity of BN-C nanostructures," Phys. Rev. B **86**, 115410.

Kittel, C., 2005, *Introduction to Solid State Physics* (Wiley, Hoboken, NJ).
Klemens, P. G., 1955, "The scattering of low-frequency lattice waves by static imperfections," Proc. Phys. Soc. London Sect. A **68**, 1113.
Klemens, P. G., 2000, "Theory of the a-plane thermal conductivity of graphite," J. Wide Bandgap Mater. **7**, 332.
Klemens, P. G., and D. F. Pedraza, 1994, "Thermal conductivity of graphite in the basal plane," Carbon **32**, 735.
Koh, Y. K., A. S. Lyons, M.-H. Bae, B. Huang, V. E. Dorgan, D. G. Cahill, and E. Pop, 2016, "Role of remote interfacial phonon (RIP) scattering in heat transport across graphene/SiO_2 interfaces," Nano Lett. **16**, 6014.
Koreeda, A., R. Takano, and S. Saikan, 2007, "Second sound in $SrTiO_3$," Phys. Rev. Lett. **99**, 265502.
Kuang, Y., L. Lindsay, and B. Huang, 2015, "Unusual enhancement in intrinsic thermal conductivity of multilayer graphene by tensile strains," Nano Lett. **15**, 6121.
Kuang, Y., L. Lindsay, S. Shi, X. Wang, and B. Huang, 2016, "Thermal conductivity of graphene mediated by strain and size," Int. J. Heat Mass Transfer **101**, 772.
Kuang, Y. D., L. Lindsay, S. Q. Shi, and G. Zheng, 2016, "Tensile strains give rise to strong size effects for thermal conductivities of silicene, germanene and stanene," Nanoscale **8**, 3760.
Kundu, A., N. Mingo, D. Broido, and D. Stewart, 2011, "Role of light and heavy embedded nanoparticles on the thermal conductivity of SiGe alloys," Phys. Rev. B **84**, 125426.
Lee, J.-U., D. Yoon, H. Kim, S. W. Lee, and H. Cheong, 2011, "Thermal conductivity of suspended pristine graphene measured by Raman spectroscopy," Phys. Rev. B **83**, 081419.
Lee, S., D. Broido, K. Esfarjani, and G. Chen, 2015, "Hydrodynamic phonon transport in suspended graphene," Nat. Commun. **6**, 6290.
Lee, S., K. Hippalgaonkar, F. Yang, J. Hong, C. Ko, J. Suh, K. Liu, K. Wang, J. J. Urban, and X. Zhang, 2017, "Anomalously low electronic thermal conductivity in metallic vanadium dioxide," Science **355**, 371.
Lee, S., *et al.*, 2015, "Anisotropic in-plane thermal conductivity of black phosphorus nanoribbons at temperatures higher than 100 K," Nat. Commun. **6**, 8573.
Lepri, S., 1998, "Relaxation of classical many-body Hamiltonians in one dimension," Phys. Rev. E **58**, 7165.
Lepri, S., R. Livi, and A. Politi, 1998, "On the anomalous thermal conductivity of one-dimensional lattices," Europhys. Lett. **43**, 271.
Lepri, S., R. Livi, and A. Politi, 2003, "Thermal conduction in classical low-dimensional lattices," Phys. Rep. **377**, 1.
Lepri, S., R. Livi, and A. Politi, 2016, *Thermal Transport in Low Dimensions*, Lecture Notes in Physics Vol. 921 (Springer, Berlin), pp. 1–37.
Li, H., H. Ying, X. Chen, D. L. Nika, A. I. Cocemasov, W. Cai, A. A. Balandin, and S. Chen, 2014, "Thermal conductivity of twisted bilayer graphene," Nanoscale **6**, 13402.
Li, H., Q. Zhang, C. C. R. Yap, B. K. Tay, T. H. T. Edwin, A. Olivier, and D. Baillargeat, 2012, "From bulk to monolayer MoS_2: evolution of Raman scattering," Adv. Funct. Mater. **22**, 1385.
Li, Q.-Y., K. Takahashi, H. Ago, X. Zhang, T. Ikuta, T. Nishiyama, and K. Kawahara, 2015, "Temperature dependent thermal conductivity of a suspended submicron graphene ribbon," J. Appl. Phys. **117**, 065102.
Li, T., 2012, "Ideal strength and phonon instability in single-layer MoS 2," Phys. Rev. B **85**, 235407.
Li, W., J. Carrete, and Natalio Mingo, 2013, "Thermal conductivity and phonon linewidths of monolayer MoS_2 from first principles," Appl. Phys. Lett. **103**, 253103.
Li, W., L. Lindsay, D. Broido, D. A. Stewart, and N. Mingo, 2012, "Thermal conductivity of bulk and nanowire $Mg_2Si_xSn_{1-x}$ alloys from first principles," Phys. Rev. B **86**, 174307.
Li, W., N. Mingo, L. Lindsay, D. A. Broido, D. A. Stewart, and N. A. Katcho, 2012, "Thermal conductivity of diamond nanowires from first principles," Phys. Rev. B **85**, 195436.
Li, X., K. Maute, M. L. Dunn, and R. Yang, 2010, "Strain effects on the thermal conductivity of nanostructures," Phys. Rev. B **81**, 245318.
Li, Z. Y., Y. Z Liu, L. Lindsay, Y. Xu, W-H. Duan, and E. Pop, 2017, "Size Dependence and Ballistic Limits of Thermal Transport in Anisotropic Layered Two-Dimensional Materials," arXiv:1711.02772.
Lindsay, L., and D. Broido, 2011, "Enhanced thermal conductivity and isotope effect in single-layer hexagonal boron nitride," Phys. Rev. B **84**, 155421.
Lindsay, L., and D. Broido, 2012, "Theory of thermal transport in multilayer hexagonal boron nitride and nanotubes," Phys. Rev. B **85**, 035436.
Lindsay, L., D. Broido, and N. Mingo, 2010a, "Diameter dependence of carbon nanotube thermal conductivity and extension to the graphene limit," Phys. Rev. B **82**, 161402.
Lindsay, L., D. Broido, and N. Mingo, 2010b, "Flexural phonons and thermal transport in graphene," Phys. Rev. B **82**, 115427.
Lindsay, L., D. Broido, and N. Mingo, 2011, "Flexural phonons and thermal transport in multilayer graphene and graphite," Phys. Rev. B **83**, 235428.
Lindsay, L., W. Li, J. Carrete, N. Mingo, D. Broido, and T. Reinecke, 2014, "Phonon thermal transport in strained and unstrained graphene from first principles," Phys. Rev. B **89**, 155426.
Lindsay, L. R., 2010, Ph.D. thesis (Boston College).
Lippi, A., and R. Livi, 2000, "Heat conduction in two-dimensional nonlinear lattices," J. Stat. Phys. **100**, 1147.
Liu, B., J. A. Baimova, C. D. Reddy, S. V. Dmitriev, W. K. Law, X. Q. Feng, and K. Zhou, 2014, "Interface thermal conductance and rectification in hybrid graphene/silicene monolayer," Carbon **79**, 236.
Liu, B., F. Meng, C. D. Reddy, J. A. Baimova, N. Srikanth, S. V. Dmitriev, and K. Zhou, 2015, "Thermal transport in a graphene–MoS_2 bilayer heterostructure: a molecular dynamics study," RSC Adv. **5**, 29193.
Liu, B., C. Reddy, J. Jiang, J. A. Baimova, S. V. Dmitriev, A. A. Nazarov, and K. Zhou, 2012, "Morphology and in-plane thermal conductivity of hybrid graphene sheets," Appl. Phys. Lett. **101**, 211909.
Liu, F., P. Ming, and J. Li, 2007, "Ab initio calculation of ideal strength and phonon instability of graphene under tension," Phys. Rev. B **76**, 064120.
Liu, H., G. Qin, Y. Lin, and M. Hu, 2016, "Disparate Strain Dependent Thermal Conductivity of Two-dimensional Penta-Structures," Nano Lett. **16**, 3831.
Liu, J., G.-M. Choi, and D. G. Cahill, 2014, "Measurement of the anisotropic thermal conductivity of molybdenum disulfide by the time-resolved magneto-optic Kerr effect," J. Appl. Phys. **116**, 233107.
Liu, J., and R. Yang, 2012, "Length-dependent thermal conductivity of single extended polymer chains," Phys. Rev. B **86**, 104307.
Liu, S., P Hänggi, N. Li, J. Ren, and B. Li, 2014, "Anomalous heat diffusion," Phys. Rev. Lett. **112**, 040601.
Liu, T.-H., Y.-C. Chen, C.-W. Pao, and C.-C. Chang, 2014, "Anisotropic thermal conductivity of MoS_2 nanoribbons: Chirality and edge effects," Appl. Phys. Lett. **104**, 201909.

Liu, X., G. Zhang, Q.-X. Pei, and Y.-W. Zhang, 2013, "Phonon thermal conductivity of monolayer MoS_2 sheet and nanoribbons," Appl. Phys. Lett. **103**, 133113.

Luo, Z., J. Maassen, Y. Deng, Y. Du, R. P. Garrelts, M. S. Lundstrom, D. Y. Peide, and X. Xu, 2015, "Anisotropic in-plane thermal conductivity observed in few-layer black phosphorus," Nat. Commun. **6**, 8572.

Mai, T., and O. Narayan, 2006, "Universality of one-dimensional heat conductivity," Phys. Rev. E **73**, 061202.

Majee, A. K. and Z. Aksamija, 2016, "Length divergence of the lattice thermal conductivity in suspended graphene nanoribbons," Phys. Rev. B **93**, 235423.

Mak, K. F., C. H. Lui, and T. F. Heinz, 2010, "Measurement of the thermal conductance of the graphene/SiO_2 interface," Appl. Phys. Lett., **97**, 221904.

Malekpour, H., P. Ramnani, S. Srinivasan, G. Balasubramanian, D. L. Nika, A. Mulchandani, R. K. Lake, and A. A. Balandin, 2016, "Thermal conductivity of graphene with defects induced by electron beam irradiation," Nanoscale **8**, 14608.

Mariani, E., and F. von Oppen, 2008, "Flexural phonons in free-standing graphene," Phys. Rev. Lett. **100**, 076801.

Maruyama, S., 2002, "A molecular dynamics simulation of heat conduction in finite length SWNTs," Physica B (Amsterdam) **323**, 193.

Mingo, N., and D. Broido, 2005, "Length dependence of carbon nanotube thermal conductivity and the "problem of long waves," Nano Lett. **5**, 1221.

Mingo, N., K. Esfarjani, D. Broido, and D. Stewart, 2010, "Cluster scattering effects on phonon conduction in graphene," Phys. Rev. B **81**, 045408.

Mohiuddin, T. M. G., *et al.*, 2009, "Uniaxial strain in graphene by Raman spectroscopy: G peak splitting, Grüneisen parameters, and sample orientation," Phys. Rev. B **79**, 205433.

Morelli, D., and J. Heremans, 2002, "Thermal conductivity of germanium, silicon, and carbon nitrides," Appl. Phys. Lett. **81**, 5126.

Mounet, N., and N. Marzari 2005, "First-principles determination of the structural, vibrational and thermodynamic properties of diamond, graphite, and derivatives," Phys. Rev. B **71**, 205214.

Mu, X., X. Wu, T. Zhang, D. B. Go, and T. Luo, 2014, "Thermal transport in graphene oxide-from ballistic extreme to amorphous limit," Sci. Rep. **4**, 3909.

Narayan, O., and S. Ramaswamy, 2002, "Anomalous heat conduction in one-dimensional momentum-conserving systems," Phys. Rev. Lett. **89**, 200601.

Narayanamurti, V., and R. Dynes, 1972, "Observation of second sound in bismuth," Phys. Rev. Lett. **28**, 1461.

Nguyen, V. H., M. C. Nguyen, H. V. Nguyen, J. Saint-Martin, and P. Dollfus, 2014, "Enhanced thermoelectric figure of merit in vertical graphene junctions," Appl. Phys. Lett., **105**, 133105.

Ni, Y., Y. Chalopin, and S. Volz, 2013, "Few layer graphene based superlattices as efficient thermal insulators," Appl. Phys. Lett., **103**, 141905.

Nika, D. L., A. S. Askerov, and A. A. Balandin, 2012, "Anomalous size dependence of the thermal conductivity of graphene ribbons," Nano Lett. **12**, 3238.

Nika, D. L., and A. A. Balandin, 2012, "Two-dimensional phonon transport in graphene," J. Phys. Condens. Matter **24**, 233203.

Nika, D. L., and A. A. Balandin, 2017, "Phonons and thermal transport in graphene and graphene-based materials," Rep. Prog. Phys. **80**, 036502.

Nika, D. L., A. I. Cocemasov, and A. A. Balandin, 2014, "Specific heat of twisted bilayer graphene: Engineering phonons by atomic plane rotations," Appl. Phys. Lett. **105**, 031904.

Nika, D. L., S. Ghosh, E. P. Pokatilov, and A. A. Balandin, 2009, "Lattice thermal conductivity of graphene flakes: Comparison with bulk graphite," Appl. Phys. Lett., **94**, 203103.

Nika, D. L., E. P. Pokatilov, A. S. Askerov, and A. A. Balandin, 2009, "Phonon thermal conduction in graphene: Role of Umklapp and edge roughness scattering," Phys. Rev. B, **79**, 155413.

Omini, M., and A. Sparavigna, 1996, "Beyond the isotropic-model approximation in the theory of thermal conductivity," Phys. Rev. B **53**, 9064.

Ong, Z.-Y., and E. Pop, 2011, "Effect of substrate modes on thermal transport in supported graphene," Phys. Rev. B **84**, 075471.

Ouyang, T., Y. Chen, L.-M. Liu, Y. Xie, X. Wei, and J. Zhong, 2012, "Thermal transport in graphyne nanoribbons," Phys. Rev. B **85**, 235436.

Ouyang, T., Y. Chen, Y. Xie, K. Yang, Z. Bao, and J. Zhong, 2010, "Thermal transport in hexagonal boron nitride nanoribbons," Nanotechnology **21**, 245701.

Palomaki, T., J. Harlow, J. Teufel, R. Simmonds, and K. Lehnert, 2013, "Coherent state transfer between itinerant microwave fields and a mechanical oscillator," Nature (London) **495**, 210.

Park, M., S.-C. Lee, and Y.-S. Kim, 2013, "Length-dependent lattice thermal conductivity of graphene and its macroscopic limit," J. Appl. Phys. **114**, 053506.

Parrish, K. D., A. Jain, J. M. Larkin, W. A. Saidi, and A. J. McGaughey, 2014, "Origins of thermal conductivity changes in strained crystals," Phys. Rev. B **90**, 235201.

Pei, Q.-X., Z.-D. Sha, and Y.-W. Zhang, 2011, "A theoretical analysis of the thermal conductivity of hydrogenated graphene," Carbon **49**, 4752.

Peimyoo, N., J. Shang, W. Yang, Y. Wang, C. Cong, and T. Yu, 2015, "Thermal conductivity determination of suspended mono-and bilayer WS2 by Raman spectroscopy," Nano Res. **8**, 1210.

Peng, B., H. Zhang, H. Shao, Y. Xu, X. Zhang, and H. Zhu, 2016, "Low lattice thermal conductivity of stanene," Sci. Rep. **6**, 20225.

Pereira, L. F. C., and D. Donadio, 2013, "Divergence of the thermal conductivity in uniaxially strained graphene," Phys. Rev. B **87**, 125424.

Pereverzev, A., 2003, "Fermi-Pasta-Ulam β lattice: Peierls equation and anomalous heat conductivity," Phys. Rev. E **68**, 056124.

Pettes, M. T., I. Jo, Z. Yao, and L. Shi, 2011, "Influence of polymeric residue on the thermal conductivity of suspended bilayer graphene," Nano Lett. **11**, 1195.

Pettes, M. T., J. Maassen, I. Jo, M. S. Lundstrom, and L. Shi, 2013, "Effects of surface band bending and scattering on thermoelectric transport in suspended bismuth telluride nanoplates," Nano Lett. **13**, 5316.

Pettes, M. T., M. R. Sadeghi, H. Ji, I. Jo, W. Wei, R. S. Ruoff, and L. Shi, 2015, "Scattering of phonons by high-concentration isotopic impurities in ultrathin graphite," Phys. Rev. B, **91**, 035429.

Picu, R., T. Borca-Tasciuc, and M. Pavel, 2003, "Strain and size effects on heat transport in nanostructures," J. Appl. Phys. **93**, 3535.

Pohl, D. W., and V. Irniger, 1976, "Observation of second sound in NaF by means of light scattering," Phys. Rev. Lett. **36**, 480.

Pop, E., V. Varshney, and A. K. Roy, 2012, "Thermal properties of graphene: Fundamentals and applications," MRS Bull. **37**, 1273.

Poudel, B., *et al.*, 2008, "High-thermoelectric performance of nanostructured bismuth antimony telluride bulk alloys," Science **320**, 634.

Prosen, T., and D. K. Campbell, 2000, "Momentum conservation implies anomalous energy transport in 1D classical lattices," Phys. Rev. Lett. **84**, 2857.

Qian, X., X. Gu, M. S. Dresselhaus, and R. G. Yang, 2016, "Anisotropic Tuning on Graphite Thermal Conductivity by Lithium Intercalation," J. Phys. Chem. Lett. **7**, 4744.

Qian, X., P. Q. Jiang, Y. Peng, X. Gu, Z. Liu, and R. G. Yang, 2018, "Anistropic Thermal Transport in van der Waals Layered Alloys $WSe_{2(1-x)}Te_{2x}$," Appl. Phys. Lett. **112**, 241901.

Qin, G., and M. Hu, 2016, in *Diverse Thermal Transport Properties of Two-Dimensional Materials: A Comparative Review*, edited by P. K. Nayak (InTech, Rijeka, Croatia).

Qin, G., Z. Qin, W.-Z. Fang, L.-C. Zhang, S.-Y. Yue, Z.-B. Yan, M. Hu, and G. Su, 2016, "Diverse anisotropy of phonon transport in two-dimensional IV-VI compounds: A comparative study," Nanoscale **8**, 11306.

Qin, G., X. Zhang, S.-Y. Yue, Z. Qin, H. Wang, Y. Han, and M. Hu, 2016, "Resonant bonding driven giant phonon anharmonicity and low thermal conductivity of phosphorene," Phys. Rev. B **94**, 165445.

Qin, T., J. Zhou, and J. Shi, 2012, "Berry curvature and the phonon Hall effect," Phys. Rev. B **86**, 104305.

Qiu, B., and X. Ruan, 2010, "Thermal conductivity prediction and analysis of few-quintuple Bi_2Te_3 thin films: A molecular dynamics study," Appl. Phys. Lett. **97**, 183107.

Qiu, B., and X. Ruan, 2012, "Reduction of spectral phonon relaxation times from suspended to supported graphene," Appl. Phys. Lett. **100**, 193101.

Ratsifaritana, C. A., and P. G. Klemens, 1987, "Scattering of phonons by vacancies," Int. J. Thermophys. **8**, 737.

Ross, R. G., P. Andersson, B. Sundqvist, and G. Backstrom, 1984, "Thermal conductivity of solids and liquids under pressure," Rep. Prog. Phys. **47**, 1347.

Sadeghi, M. M., I. Jo, and L. Shi, 2013, "Phonon-interface scattering in multilayer graphene on an amorphous support," Proc. Natl. Acad. Sci. U.S.A. **110**, 16321.

Sadeghi, M. M., M. T. Pettes, and L. Shi, 2012, "Thermal transport in graphene," Solid State Commun. **152**, 1321.

Sahoo, S., A. P. Gaur, M. Ahmadi, M. J.-F. Guinel, and R. S. Katiyar, 2013, "Temperature-dependent Raman studies and thermal conductivity of few-layer MoS_2," J. Phys. Chem. C **117**, 9042.

Sato, D. S., 2016, "Pressure-induced recovery of Fourier's law in one-dimensional momentum-conserving systems," Phys. Rev. E **94**, 012115.

Savin, V., and Y. A. Kosevich, 2014, "Thermal conductivity of molecular chains with asymmetric potentials of pair interactions," Phys. Rev. E **89**, 032102.

Schmidt, A. J., X. Chen, and G. Chen, 2008, "Pulse accumulation, radial heat conduction, and anisotropic thermal conductivity in pump-probe transient thermoreflectance," Rev. Sci. Instrum. **79**, 114902.

Seol, J. H., *et al.*, 2010, "Two-dimensional phonon transport in supported graphene," Science **328**, 213.

Sevik, C., A. Kinaci, J. B. Haskins, and T. Çağın, 2011, "Characterization of thermal transport in low-dimensional boron nitride nanostructures," Phys. Rev. B **84**, 085409.

Sevinçli, H., W. Li, N. Mingo, G. Cuniberti, and S. Roche, 2011, "Effects of domains in phonon conduction through hybrid boron nitride and graphene sheets," Phys. Rev. B **84**, 205444.

Shi, L., D. Li, C. Yu, W. Jang, D. Kim, Z. Yao, P. Kim, and A. Majumdar, 2003, "Measuring thermal and thermoelectric properties of one-dimensional nanostructures using a microfabricated device," J. Heat Transfer **125**, 881.

Singh, D., J. Y. Murthy, and T. S. Fisher, 2011, "Mechanism of thermal conductivity reduction in few-layer graphene," J. Appl. Phys. **110**, 044317.

Singh, V., S. Bosman, B. Schneider, Y. M. Blanter, A. Castellanos-Gomez, and G. Steele, 2014, "Optomechanical coupling between a multilayer graphene mechanical resonator and a superconducting microwave cavity," Nat. Nanotechnol. **9**, 820.

Slack, G. A., 1973, "Nonmetallic crystals with high thermal conductivity," J. Phys. Chem. Solids **34**, 321.

Song, J., and N. V. Medhekar, 2013, "Thermal transport in lattice-constrained 2D hybrid graphene heterostructures," J. Phys. Condens. Matter **25**, 445007.

Strohm, C., G. Rikken, and P. Wyder, 2005, "Phenomenological evidence for the phonon Hall effect," Phys. Rev. Lett. **95**, 155901.

Sullivan, S., A. Vallabhaneni, I. Kholmanov, X. Ruan, J. Murthy, and L. Shi, 2017, "Optical generation and detection of local non-equilibrium phonons in suspended graphene," Nano Lett. **17**, 2049.

Sun, B., X. Gu, Q. Zeng, X. Huang, Y. Yan, Z. Liu, R. Yang, and Y. K. Koh, 2017, "Temperature Dependence of Anisotropic Thermal-Conductivity Tensor of Bulk Black Phosphorus," Adv. Mater. **29**, 1603297.

Tamura, S.-i., 1983, "Isotope scattering of dispersive phonons in Ge," Phys. Rev. B **27**, 858.

Tan, Z. W., J.-S. Wang, and C. K. Gan, 2011, "First-principles study of heat transport properties of graphene nanoribbons," Nano Lett. **11**, 214.

Tang, X., S. Xu, J. Zhang, and X. Wang, 2014, "Five orders of magnitude reduction in energy coupling across corrugated graphene/substrate interfaces," ACS Appl. Mater. Interfaces **6**, 2809.

Taube, A., J. Judek, A. Łapińska, and M. Zdrojek, 2015, "Temperature-dependent thermal properties of supported MoS_2 monolayers," ACS Appl. Mater. Interfaces **7**, 5061.

Teweldebrhan, D., V. Goyal, and A. A. Balandin, 2010, "Exfoliation and characterization of bismuth telluride atomic quintuples and quasi-two-dimensional crystals," Nano Lett. **10**, 1209.

Tian, L., 2015, "Optoelectromechanical transducer: Reversible conversion between microwave and optical photons," Ann. Phys. (Berlin) **527**, 1.

Tran, V. T., J. Saint-Martin, P. Dollfus, and S. Volz, 2017, "Optimizing the thermoelectric performance of graphene nanoribbons without degrading the electronic properties," Sci. Rep., **7**, 2313.

Vallabhaneni, A. K., D. Singh, H. Bao, J. Murthy, and X. Ruan, 2016, "Reliability of Raman measurements of thermal conductivity of single-layer graphene due to selective electron-phonon coupling: A first-principles study," Phys. Rev. B **93**, 125432.

Venkatasubramanian, R., E. Siivola, T. Colpitts, and B. O'quinn, 2001, "Thin-film thermoelectric devices with high room-temperature figures of merit," Nature (London) **413**, 597.

Wan, C., *et al.*, 2015, "Flexible n-type thermoelectric materials by organic intercalation of layered transition metal dichalcogenide TiS_2," Nat. Mater. **14**, 622.

Wan, C., Y. Kodama, M. Kondo, R. Sasai, X. Qian, X. Gu, K. Koga, K. Yabuki, R. Yang, and K. Koumoto, 2015, "Dielectric mismatch mediates carrier mobility in organic-intercalated layered TiS_2," Nano Lett. **15**, 6302.

Wan, C., Y. Wang, W. Norimatsu, M. Kusunoki, and K. Koumoto, 2012, "Nanoscale stacking faults induced low thermal conductivity in thermoelectric layered metal sulfides," Appl. Phys. Lett. **100**, 101913.

Wan, C., Y. Wang, N. Wang, and K. Koumoto, 2010, "Low-thermal-conductivity $(MS)_{1+x}(TiS_2)_2$ (M = Pb, Bi, Sn) misfit layer compounds for bulk thermoelectric materials," Materials **3**, 2606.
Wan, C., Y. Wang, N. Wang, W. Norimatsu, M. Kusunoki, and K. Koumoto, 2010, "Development of novel thermoelectric materials by reduction of lattice thermal conductivity," Sci. Technol. Adv. Mater. **11**, 044306.
Wan, C., Y. Wang, N. Wang, W. Norimatsu, M. Kusunoki, and K. Koumoto, 2011, "Intercalation: building a natural superlattice for better thermoelectric performance in layered Chalcogenides," J. Electron. Mater. **40**, 1271.
Wang, F. Q., S. Zhang, J. Yu, and Q. Wang, 2015, "Thermoelectric properties of single-layered SnSe sheet," Nanoscale **7**, 15962.
Wang, H., and M. S. Daw, 2016, "Anharmonic renormalization of the dispersion of flexural modes in graphene using atomistic calculations," Phys. Rev. B **94**, 155434.
Wang, J. Y., 2013, Ph.D. thesis (National University of Singapore).
Wang, L., B. Hu, and B. Li, 2012, "Logarithmic divergent thermal conductivity in two-dimensional nonlinear lattices," Phys. Rev. E **86**, 040101.
Wang, Li, B. Hu, and B. Li, 2013, "Validity of Fourier's law in one-dimensional momentum-conserving lattices with asymmetric interparticle interactions," Phys. Rev. E **88**, 052112.
Wang, Y., B. Qiu, and X. Ruan, 2012, "Edge effect on thermal transport in graphene nanoribbons: A phonon localization mechanism beyond edge roughness scattering," Appl. Phys. Lett. **101**, 013101.
Wang, Y., A. K. Vallabhaneni, B. Qiu, and X. Ruan, 2014, "Two-dimensional thermal transport in graphene: a review of numerical modeling studies," Nanoscale Micro. Thermophys. Eng. **18**, 155.
Wang, Y., N. Xu, D. Li, and J. Zhu, 2017, "Thermal Properties of Two Dimensional Layered Materials," Adv. Funct. Mater. **27**, 1604134.
Ward, A., D. Broido, D. A. Stewart, and G. Deinzer, 2009, "Ab initio theory of the lattice thermal conductivity in diamond," Phys. Rev. B **80**, 125203.
Wei, N., L. Xu, H.-Q. Wang, and J.-C. Zheng, 2011, "Strain engineering of thermal conductivity in graphene sheets and nanoribbons: a demonstration of magic flexibility," Nanotechnology **22**, 105705.
Wei, Y., B. Wang, J. Wu, R. Yang, and M. L. Dunn, 2013, "Bending rigidity and Gaussian bending stiffness of single-layered graphene," Nano Lett. **13**, 26.
Wei, Z., Y. Chen, and C. Dames, 2012, "Wave packet simulations of phonon boundary scattering at graphene edges," J. Appl. Phys. **112**, 024328.
Wei, Z., Z. Ni, K. Bi, M. Chen, and Y. Chen, 2011, "In-plane lattice thermal conductivities of multilayer graphene films," Carbon **49**, 2653.
Wei, Z., J. Yang, K. Bi, and Y. Chen, 2014, "Mode dependent lattice thermal conductivity of single layer graphene," J. Appl. Phys. **116**, 153503.
Wei, Z., J. Yang, W. Chen, K. Bi, D. Li, and Y. Chen, 2014, "Phonon mean free path of graphite along the c-axis," Appl. Phys. Lett. **104**, 081903.
Whittingham, M. S., and A. J. Jacobson, 1982, *Intercalation Chemistry* (Academic Press, New York).
Wilson, J., and A. Yoffe, 1969, "The transition metal dichalcogenides discussion and interpretation of the observed optical, electrical and structural properties," Adv. Phys. **18**, 193.
Xie, G., Y. Shen, X. Wei, L. Yang, H. Xiao, J. Zhong, and G. Zhang, 2014, "A Bond-order Theory on the Phonon Scattering by Vacancies in Two-dimensional Materials," Sci. Rep. **4**, 5085.
Xie, H., L. Chen, W. Yu, and B. Wang, 2013, "Temperature dependent thermal conductivity of a free-standing graphene nanoribbon," Appl. Phys. Lett. **102**, 111911.
Xie, H., T. Ouyang, É. Germaneau, G. Qin, M. Hu, and H. Bao, 2016, "Large tunability of lattice thermal conductivity of monolayer silicene via mechanical strain," Phys. Rev. B **93**, 075404.
Xiong, D., J. Wang, Y. Zhang, and H. Zhao, 2010, "Heat conduction in two-dimensional disk models," Phys. Rev. E **82**, 030101.
Xu, X., J. Chen, and B. Li, 2016, "Phonon thermal conduction in novel 2D materials," J. Phys. Condens. Matter **28**, 483001.
Xu, X., L. F. Pereira, Y. Wang, J. Wu, K. Zhang, X. Zhao, S. Bae, C. T. Bui, R. Xie, and J. T. Thong, 2014, "Length-dependent thermal conductivity in suspended single-layer graphene," Nat. Commun. **5**, 3689.
Xu, Y., X. Chen, B.-L. Gu, and W. Duan, 2009, "Intrinsic anisotropy of thermal conductance in graphene nanoribbons," Appl. Phys. Lett. **95**, 233116.
Xu, Y., and G. Li, 2009, "Strain effect analysis on phonon thermal conductivity of two-dimensional nanocomposites," J. Appl. Phys. **106**, 114302.
Xu, Y., Z. Li, and W. Duan, 2014, "Thermal and thermoelectric properties of graphene," Small **10**, 2182.
Xu, Z., and M. J. Buehler, 2009, "Strain controlled thermomutability of single-walled carbon nanotubes," Nanotechnology **20**, 185701.
Yan, J.-A., W. Y. Ruan, and M. Y. Chou, 2008, "Phonon dispersions and vibrational properties of monolayer, bilayer, and trilayer graphene: Density-functional perturbation theory," Phys. Rev. B **77**, 125401.
Yan, R., J. R. Simpson, S. Bertolazzi, J. Brivio, M. Watson, X. Wu, A. Kis, T. Luo, A. R. Hight Walker, and H. G. Xing, 2014, "Thermal conductivity of monolayer molybdenum disulfide obtained from temperature-dependent Raman spectroscopy," ACS Nano **8**, 986.
Yan, X.-J., Y.-Y. Lv, L. Li, X. Li, S.-H. Yao, Y.-B. Chen, X.-P. Liu, H. Lu, M.-H. Lu, and Y.-F. Chen, 2017, "Composition dependent phase transition and its induced hysteretic effect in the thermal conductivity of $W_xMo_{1-x}Te_2$," Appl. Phys. Lett. **110**, 211904.
Yan, Z., C. Jiang, T. Pope, C. Tsang, J. Stickney, P. Goli, J. Renteria, T. Salguero, and A. Balandin, 2013, "Phonon and thermal properties of exfoliated $TaSe_2$ thin films," J. Appl. Phys. **114**, 204301.
Yang, J., E. Ziade, C. Maragliano, R. Crowder, X. Wang, M. Stefancich, M. Chiesa, A. K. Swan, and A. J. Schmidt, 2014, "Thermal conductance imaging of graphene contacts," J. Appl. Phys. **116**, 023515.
Yang, L., P. Grassberger, and B. Hu, 2006, "Dimensional crossover of heat conduction in low dimensions," Phys. Rev. E **74**, 062101.
Yang, N., X. Xu, G. Zhang, and B. Li, 2012, "Thermal transport in nanostructures," AIP Adv. **2**, 041410.
Yang, N., G. Zhang, and B. Li, 2010, "Violation of Fourier's law and anomalous heat diffusion in silicon nanowires," Nano Today **5**, 85.
Yang, R., and G. Chen, 2004, "Thermal conductivity modeling of periodic two-dimensional nanocomposites," Phys. Rev. B **69**, 195316.
Yang, R., G. Chen, and M. S. Dresselhaus, 2005, "Thermal conductivity of simple and tubular nanowire composites in the longitudinal direction," Phys. Rev. B **72**, 125418.
Ye, Z.-Q., B.-Y. Cao, W.-J. Yao, T. Feng, and X. Ruan, 2015, "Spectral phonon thermal properties in graphene nanoribbons," Carbon **93**, 915.
Zabel, H., 2001, "Phonons in layered compounds," J. Phys. Condens. Matter **13**, 7679.

Zeraati, M., S. M. V. Allaei, I. A. Sarsari, M. Pourfath, and D. Donadio, 2016, "Highly anisotropic thermal conductivity of arsenene: An ab initio study," Phys. Rev. B **93**, 085424.

Zhang, G., and B. Li, 2005, "Thermal conductivity of nanotubes revisited: Effects of chirality, isotope impurity, tube length, and temperature," J. Chem. Phys. **123**, 114714.

Zhang, G., and Y.-W. Zhang, 2017, "Thermal properties of two-dimensional materials," Chin. Phys. B **26**, 034401.

Zhang, H., X. Chen, Y.-D. Jho, and A. J. Minnich, 2016, "Temperature-Dependent Mean Free Path Spectra of Thermal Phonons Along the c-Axis of Graphite," Nano Lett. **16**, 1643.

Zhang, H., G. Lee, and K. Cho, 2011, "Thermal transport in graphene and effects of vacancy defects," Phys. Rev. B **84**, 115460.

Zhang, H., C.-X. Liu, X.-L. Qi, X. Dai, Z. Fang, and S.-C. Zhang, 2009, "Topological insulators in Bi_2Se_3, Bi_2Te_3 and Sb_2Te_3 with a single Dirac cone on the surface," Nat. Phys. **5**, 438.

Zhang, J., Y. Hong, and Y. Yue, 2015, "Thermal transport across graphene and single layer hexagonal boron nitride," J. Appl. Phys. **117**, 134307.

Zhang, L., J. Ren, J.-S. Wang, and B. Li, 2010, "Topological nature of the phonon Hall effect," Phys. Rev. Lett. **105**, 225901.

Zhang, X., D. Sun, Y. Li, G.-H. Lee, X. Cui, D. Chenet, Y. You, T. F. Heinz, and J. C. Hone, 2015, "Measurement of lateral and interfacial thermal conductivity of single-and bilayer MoS_2 and $MoSe_2$ using refined optothermal raman technique," ACS Appl. Mater. Interfaces **7**, 25923.

Zhang, Z.-W., S.-Q. Hu, J. Chen, and B. Li, 2017, "Hexagonal Boron nitride: A promising substrate for graphene with high heat dissipation," Nanotechnology **28**, 226704.

Zhong, W.-R., M.-P. Zhang, B.-Q. Ai, and D.-Q. Zheng, 2011, "Chirality and thickness-dependent thermal conductivity of few-layer graphene: a molecular dynamics study," Appl. Phys. Lett. **98**, 113107.

Zhong, Y., Y. Zhang, J. Wang, and H. Zhao, 2012, "Normal heat conduction in one-dimensional momentum conserving lattices with asymmetric interactions," Phys. Rev. E **85**, 060102.

Zhu, G., J. Liu, Q. Zheng, R. Zhang, D. Li, D. Banerjee, and D. G. Cahill, 2016, "Tuning thermal conductivity in molybdenum disulfide by electrochemical intercalation," Nat. Commun. **7**, 13211.

Zhu, J., *et al.*, 2016, "Revealing the Origins of 3D Anisotropic Thermal Conductivities of Black Phosphorus," Adv. Electron. Mater. **2**, 1600040.

Zhu, L., G. Zhang, and B. Li, 2014, "Coexistence of size-dependent and size-independent thermal conductivities in phosphorene," Phys. Rev. B **90**, 214302.

Zhu, T., and E. Ertekin, 2014, "Phonon transport on two-dimensional graphene/boron nitride superlattices," Phys. Rev. B **90**, 195209.

Ziman, J. M., 1960, *Electrons and phonons: the theory of transport phenomena in solids* (Oxford University Press, New York).